Rapidly evolving protointrons in *Saccharomyces* genomes revealed by a hungry spliceosome

Jason Talkish, Haller Igel, Rhonda J. Perriman, Lily Shiue, Sol Katzman[1], Elizabeth M. Munding, Robert Shelansky[1], John Paul Donohue, and Manuel Ares, Jr.*

Center for Molecular Biology of RNA
Department of Molecular, Cell & Developmental Biology
[1]Department of Biomolecular Engineering
University of California, Santa Cruz
Santa Cruz, CA 95064

*Corresponding author
ares@ucsc.edu (MA)
(831) 459-4628

Abstract

Introns are a prevalent feature of eukaryotic genomes, yet their origins and contributions to genome function and evolution remain mysterious. In budding yeast, repression of the highly transcribed intron-containing ribosomal protein genes (RPGs) globally increases splicing of non-RPG transcripts through reduced competition for the spliceosome. We show that under these "hungry spliceosome" conditions, splicing occurs at more than 150 previously unannotated locations we call protointrons that do not overlap known introns. Protointrons use a less constrained set of splice sites and branchpoints than standard introns, including in one case AT-AC in place of GT-AG. Protointrons are not conserved in all closely related species, suggesting that most are not under selection. Some are found in non-coding RNAs (e. g. CUTs and SUTs), where they may contribute to the creation of new genes. Others are found across boundaries between noncoding and coding sequences, or within coding sequences, where they offer pathways to the creation of new protein variants, or new regulatory controls for existing genes. We define protointrons as (1) nonconserved intron-like sequences that are (2) infrequently spliced, and importantly (3) are not currently understood to contribute to gene expression or regulation in the way that standard introns function. A very few protointrons in *S. cerevisiae* challenge this classification by their increased splicing frequency and potential function, consistent with the proposed evolutionary process of "intronization", whereby new standard introns are created. This snapshot of intron evolution highlights the important role of the spliceosome in the expansion of transcribed genomic sequence space, providing a pathway for the rare events that may lead to the birth of new eukaryotic genes and the refinement of existing gene function.

Author Summary

The protein coding information in eukaryotic genes is broken by intervening sequences called introns that are removed from RNA during transcription by a large protein-RNA complex called the spliceosome. Where introns come from and how the spliceosome contributes to genome evolution are open questions. In this study, we find more than 150 new places in the yeast genome that are recognized by the spliceosome and spliced out as introns. Since they appear to have arisen very recently in evolution by sequence drift and do not appear to contribute to gene expression or its regulation, we call these protointrons. Protointrons are found in both protein-coding and non-coding RNAs and are not efficiently removed by the splicing machinery. Although most protointrons are not conserved, a few are spliced more efficiently, and are located where they might begin to play functional roles in gene expression, as predicted by the proposed process of intronization. The challenge now is to understand how spontaneously appearing splicing events like protointrons might contribute to the creation of new genes, new genetic controls, and new protein isoforms as genomes evolve.

Introduction

Eukaryotic genes are often split by intervening sequences called introns that are removed during and after transcription by the spliceosome and associated splicing proteins. Although much is known about the biochemical mechanisms of intron recognition and splicing [1-3], a clear understanding of the events and processes that explain the appearance and persistence of introns during the evolution of eukaryotic genomes remains elusive [4, 5].

As a necessary step in the expression of most extant eukaryotic genes, splicing has been exploited by evolution in at least two main ways. One allows diversification of the structure and function of the RNA and protein products of a gene by producing multiple distinct mRNAs through alternative splicing [2]. A second allows changes in gene expression through nonsense-mediated decay (NMD), whereby alternative splicing can lead to either functional mRNA, or to transcripts with premature stop codons that are degraded, providing developmental on-off control, or stable homeostatic expression settings [2]. The complex gene architecture of multicellular organisms, as contrasted with the simpler gene architecture in many single-celled eukaryotes, has prompted widespread speculation that alternative splicing is responsible for emergent complexity in metazoans. Although it contributes in complex and critical ways to gene function and regulation in extant eukaryotes, how splicing came to reside so pervasively in the eukaryotic lineage remains to be explained [4-6].

Until recently, gain or loss of introns has been detected by comparing closely related genomes. Many such “presence/absence” variations are inferred to be intron loss, in which reverse transcription of a spliced RNA, followed by homologous recombination of the intronless cDNA back into the gene of origin, erases the intron [6, 7]. Several mechanisms for the gain of new introns have been proposed (for review see [8, 9]). For example, single nucleotide changes that create new splice

sites (and thus new introns) can lead to "intron sliding" or new alternative splicing events [10]. "Exonization" of an Alu sequence in a large intron can lead to inclusion of a new exon and splitting of an intron into two smaller introns [11]. These intron gain mechanisms rely on pre-existing local splicing events, and represent intron diversification, rather than de novo intron creation at sites where no intron previously existed.

De novo intron creation appears to occur by two main pathways, "intron transposition" whereby an intron at one location is copied and inserted at a new location, and "intronization". First described in the marine alga *Micromonas* [12], transposition of introns called "Introner Elements" appears to have expanded an intron repeat family in some lineages [13-17] perhaps through an "armed spliceosome" carrying an intron-lariat RNA which is then reverse spliced into an mRNA (which then must be converted to cDNA to return to the genome at a new location, [6, 9]). More recently, intron transposition through an RNA intermediate has been documented in *S. cerevisiae*, supporting the idea that reverse splicing may operate to spread introns [18]. Other models suggest that introns transposition may arise by the action of DNA damage repair [19] or non-autonomous DNA transposons [20].

A distinct pathway for *de novo* intron creation is called "intronization" whereby mutations arise either through drift [4, 8, 21], or other sequence changes [22] to create sequences recognized as introns by the splicing machinery. As a genome sequence distant from other introns drifts, it may accumulate mutations that by chance allow its transcripts to be recognized by the splicing machinery and spliced. This process is thought to occur gradually over evolutionary time, generating sequences that exhibit properties of both exons and introns that are often alternatively spliced through several, different, weak splicing signals [4, 23]. Whether these sequences evolve to become bona fide introns depends on whether their removal through splicing provides a fitness advantage.

Splicing in the *S. cerevisiae* genome appears to have been streamlined by evolution, such that about 5% of genes have introns, and most that do have only one. Despite their scarcity in genes, introns appear in about 25% of transcripts when cells are growing in rich medium [24, 25]. More than a third of annotated introns are found in genes for ribosome biogenesis (ribosomal protein genes, RPGs), and their mRNAs account for 90% of the splicing performed in rapidly growing cells [25, 26]. This unusual distribution of introns in a highly expressed class of genes with shared function presents both challenges and opportunities for studying integration of splicing into core cellular regulation. For example, repressing transcription of the RPGs increases the efficiency of splicing for the majority of non-RPG introns and can suppress temperature-sensitive spliceosomal protein mutations [27, 28]. Based on this we proposed that relieving pre-mRNA competition by reducing RPG expression frees the spliceosome to process less competitive, splicing substrates it normally ignores. This phenomenon has been shown to contribute to the efficiency of meiotic splicing [28, 29], as well as regulation of Coenzyme Q_6 synthesis [30], whereby regulated repression of RPGs potentiates splicing control mechanisms at other genes.

In this study, we use rapamycin to repress RPGs and create hungry spliceosome conditions in three related yeast species that have diverged over ~10-20 million years [31], and find 163 locations in the *S. cerevisiae* genome that are substrates of the spliceosome, but distinct from the current set of annotated introns. Other studies have also found undocumented splicing events in yeast [32-39], including alternative splicing of known introns. Here we focus strictly on splicing events not associated with a known intron, which we call protointrons. To better understand intron creation, we distinguish, standard introns from protointrons as follows. Standard introns are efficiently spliced under normal growth conditions (median efficiency ~93% spliced), highly conserved in related *Saccharomyces* species, and have known functions in gene expression (93% reside in protein coding

126 regions). Protointrons on the other hand generally splice with very low efficiency (median efficiency
127 ~1% spliced), are often specific to different *Saccharomyces* species, and most importantly do not
128 have a clear role in correct gene expression. These protointrons are found in mRNAs as well as
129 noncoding RNAs such as promoter-associated transcripts, CUTs, SUTs, XUTs and other noncoding
130 RNAs [40-48]. Related yeasts *S. bayanus* and *S. mikatae* also have protointrons, but most are
131 species-specific, indicating that protointrons appear and disappear during evolution. This suggests
132 that protointrons arise initially through genetic drift and provide the raw material for intronization in
133 order to enable intron creation through a mechanism that is distinct from gene duplication or intron
134 transposition [4]. While only a very tiny fraction of protointrons might ever evolve into new
135 standard introns, we observe several, more efficiently spliced protointrons that appear to be more
136 advanced along the intronization pathway. This intermediate class of introns tend to occur in
137 5'UTRs where they might buffer the negative effects of RNA secondary structure or micro-ORFs
138 (uORFs) on translation, however there is currently no evidence that these have any adaptive value.
139 This work reveals the extent to which the spliceosome recognizes and splices intron-like sequences,
140 thus expanding the information contained in the genome. This contribution of the spliceosome to the
141 information content of the transcriptome may enhance the rate at which new genes and regulatory
142 mechanisms appear in eukaryotes.
143

144 ## Results

145 **Deeper RNA sequencing of a nonsense-mediated decay deficient strain confirms a class of rare**
146 **splicing events in *Saccharomyces cerevisiae***

147 In experiments where we observed increases in splicing efficiency of standard introns after
148 repression of RPG expression [28], we also observed unannotated splicing events, distinct from

149 known introns, whose splicing efficiency improved. In addition, inventive new RNAseq methods
150 designed to capture branchpoints [32, 34] have provided evidence for splicing events elsewhere in
151 the transcriptome. Some of these events appear to be activated in response to stress [32], which
152 down-regulates RPG expression and creates hungry spliceosome conditions. Still others are more
153 readily detected during meiosis [32, 39], or when cells are deleted for RNA decay pathway
154 components that degrade unstable transcripts [32, 33, 38]. Our interest in understanding the
155 evolution of splicing prompted us to focus on these distinct new introns. To capture more of them,
156 we obtained additional RNAseq data that included non-polyadenylated RNAs and RNAs sensitive to
157 nonsense-mediated decay. We made four libraries, one each from rRNA-depleted RNA from
158 untreated (0 min) and rapamycin treated (blocks nutrient signaling and represses RPGs, 60 min)
159 replicate cultures of a yeast strain deficient in NMD (*upf1Δ*, [49]). We obtained more than 300
160 million reads that show excellent between-replicate coherence in gene expression changes (Fig.
161 S1A). These data confirm our previous observation [28] that splicing of a majority of standard
162 introns in non-RPGs increases after rapamycin treatment. A splicing index relating change in the
163 ratio of junction/intron reads over time (SJ index = log2[junctions-t60/intron-t60] – log2[junctions-
164 t0/intron-t0]) increases for most introns in transcripts whose total transcript levels change less than
165 two-fold during the experiment (Fig 1A, blue circles, Table S1, NB: RPGs are repressed >2 fold and
166 are excluded). In addition to the standard introns, we observe more than 600 splicing events that
167 result from use of alternative 3' or 5' splice sites overlapping the standard introns (see also the study
168 by Douglass et al. [38]). Some of these splicing events have been previously characterized [33, 36,
169 37], and produce out of frame mRNAs that are more easily detected in the *upf1Δ* strain due to the
170 loss of NMD (Table S2). Because our interest here is in introns appearing at novel locations, we
171 have not studied the splicing events that overlap the standard introns any further. At this sequencing

172 depth, a set of splicing events that do not overlap any standard intron is evident (Table 1 and Table
173 S3). These are supported by reads that span sequences with known characteristics of introns but
174 occur at much lower frequencies than those for standard introns. As is the case for standard introns,
175 splicing of the majority of these nonstandard introns increases upon rapamycin treatment (Fig 1A,
176 orange circles, positive values indicate increased splicing), suggesting they are also in competition
177 with RPG pre-mRNAs for the spliceosome.
178
179 **Table 1. Easily detectable protointrons in *Saccharomyces cerevisiae upf1Δ* mutant cells**

Gene	Overlapping Junctions	5′SS	Consv 5'SS	BP (predicted)	Consv BP	3'SS	Consv 3'SS	% Spliced 0 min.	% Spliced 60 min.
MTR2	5	GTACGT GTATGT	0.04 0.00	AACTAATA AACTAACC	0.02 0.00	CAG CAG TAG	0.42 0.03 0.00	57	62
Opposing *YPL216W*	2	GTATGA GTTTGT	0.79 0.00	TACTAACA	0.77	AAG	0.16 0.14	22	35
MCR1	5	GTACGT GTACTC	0.74 0.01	TACTAAC AACTAACA TACTAACG	0.00 0.25 0.01	AAG TAG CAG	0.38 0.03 0.04	36	46
YEL023C	1	GTATGG	0.00	CACTAACA	0.27	TAG	0.41 0.18	23	17
ZTA1	2	GTATGA	0.95	TACTAATC	0.57	CAG AAG	0.98 0.99	1.6	5.3
PDX3	0	GTATCA	1.00	TACTGACG	0.50	AAG	1.00	1.6	1.9
TVP15	1	GTATGC	0.98	TACTAAGT	0.16	CAG TAG	0.62 0.62	2.2	4.7
PUS7	3	GTAAGG	0.99	TACTAACA	0.89	AAG TAG AAG AAG	0.97 0.62 0.62 0.96	6.5	4.4
YDR336W	1	GTACGT	0.06	CACTAAAA	0.12	TAG AAG	0.02 0.08	18	44
NTH1	1	GTATGG	0.99	TGCTAACA	1.00	CAG TAG	1.00 1.00	1.4	4.0
SPO1	0	GTATGT	0.52	TATTAACC	0.96	CAG	0.66	6.8	14
MCA1	0	GTACAG	0.02	GACTAATG	0.97	AAG	0.68	2.7	2.5
Opposing *IPT1*	1	GTAAGT	0.37	TACTAACT	0.25	AAG CAG	0.44 0.29	0.11	18
PDC1	1	GTATGT	1.00	CACTGACA	1.00	CAG	1.00 1.00	0.03	0.05
Downstream of *PDR12*	1	GTGTGT	0.01	GACTAACA	0.04	CAG AAG	0.00 0.02	36	31

SYN8	2	GTATGG	0.99	AACTAATA	0.23	TAG CAG CAG	0.96 0.95 0.96	2.1	3.4

Identification and validation of protointrons

To extract and validate nonstandard splicing locations from the RNAseq data, we inspected reads that span and are missing genomic sequences bounded by GT or GC on the 5' side and AG on the 3' side, aggressively filtering out those that were unlikely to have been generated by the spliceosome (Table S4, see also Methods). For example, we ignored reads that are abundant in only one library due to spurious PCR-derived "jackpot" amplification, or that are incorrectly mapped as spliced over naturally repeated sequences. We also filtered out reads that appeared fewer than three times, spanned sequences with no discernable match to a relaxed and appropriately positioned branchpoint consensus sequence (RYURAY, >45 from a 5'ss, >7 from a 3'ss), or that use a GAG 3' ss (although some of these may be true). Finally, in order to focus on new intron locations, we separated out reads that overlap known standard introns (these are found in Table S2). Finally, we merged overlapping alternative splice sites observed at each new intron location into one. From this sequencing experiment, we identify 226 splicing events at 163 intron locations in the *Saccharomyces cerevisiae* genome that do not overlap with standard introns. We call these protointrons (Table 1 and Table S3, NB: we have reclassified some previously annotated introns as protointrons based on their less efficient splicing and lack of conservation in close relatives, see below).

To characterize protointrons as a distinct class of splicing events, we inspected the alignments of many individual protointrons (for example Fig 1B) and validated more than a dozen of them by RT-PCR, cloning, and Sanger sequencing (Fig 1B and C, Table S5). These events map to a diversity of transcribed locations, including mRNAs, a variety of non-coding RNAs (CUTs, SUTs, XUTs, etc.), and within telomeric Y' repeats. 39% of protointrons can be found entirely within a

coding region (e. g. *TAF13* Fig 1B, C, Fig S1B and E), whereas others reside in noncoding regions or within RNA antisense to a standard gene (29%, e. g. *antiASH1*, Fig 1B, C, Fig S1B and C). Often alternative splice sites are observed, for example in the noncoding RNA *XUT12R-370* antisense to *TUS1* (Fig 1B, note only the product derived from use of the downstream 3' ss is visible on the gel in Fig 1C, Fig S1D). An internally initiating RNA from the meiotic *SPO1* gene expressed only during vegetative growth has a protointron (Fig 1C, Fig S1F). Protointrons can also be found crossing boundaries from the coding region to either UTR in mRNAs (17% in 5'UTR^coding; 1% in coding^3'UTR), and still others can be found completely within a UTR (9% in 5'UTR; 4% in 3'UTR). In many cases, excision, cloning and sequencing the faint band near the size predicted by the RNAseq reads identifies additional alternatively spliced forms not observed by RNAseq. For the four events shown in Fig 1C, we successfully confirmed splice junctions indicated by RNAseq (Table S3).

Several of the protointrons predicted by the RNAseq data appear to use unusual 5' splice sites (5' ss) not anticipated by examination of standard introns. Standard intron 5' ss show strong conservation of the G residue at position 5 (G5, underlined here: GUAYGU), which contributes to intron recognition through interactions first with U1 snRNA and later with U6 snRNA [50, 51]. The 5' ss consensus in mammals has a less strongly conserved G5, and a subset of mammalian introns use G at position 6 instead [52]. Validation tests of several protointrons whose 5' ss lack G5 show that they are authentic products of splicing (Fig 1D, Fig S1G). During this effort we also detected splicing at an AT-AC junction in the noncoding RNA *SUT635* (Fig 1E). Although yeast does not have a minor (U12) spliceosome, some major (U2) spliceosomal introns use AT-AC junctions [53], and mutation of a standard yeast intron shows that AT-AC is the most efficient splice junction dinucleotide combination after GT-AG [54]. Alternative AT-AC junction use has been reported for

the standard intron (a normal GT-AG intron) in *RPL30* [32], however no standard yeast intron uses AT-AC junctions normally. The appearance of an AT-AC protointron in *SUT635* suggests that AT-AC introns may represent an alternative path to evolution of standard introns.

Distinct features of protointrons: sequence, conservation, size, and splicing efficiency

To begin contrasting the features of protointrons and standard introns, we evaluated evolutionary conservation, the most obvious difference. To analyze conservation around splicing signals of both intron classes, we extracted a sequence window surrounding the 5'ss, predicted branchpoint, and 3'ss from each standard intron and protointron and compared them. Position-specific weight matrix-based logos of the splicing signals (Fig 2A) reveal that protointrons use a more divergent collection of splicing signals than do standard introns. As noted above, G5 of the 5'ss is a prominent feature of the standard yeast intron 5'ss but is less well represented among protointron 5'ss. Similarly, the predicted branchpoint sequences of protointrons lack strong representation of bases to either side of the core CUAA of the UACUAAC consensus for standard introns. Branchpoints of standard introns are enriched for Us upstream of the consensus and for A just downstream, and neither of these context elements are prominent in the predicted branchpoints of protointrons. The 3'ss are more similar, but as with the branchpoint, the U-rich context detectable upstream of the standard intron 3'ss is not observed in protointrons. The more diverse collection of splicing signals used by protointrons is similar to that of the overlapping alternative splice sites of standard introns [33], and a mixed set of overlapping and distinct potential introns detected using a branchpoint sequencing approach [32]. Furthermore, we note that protointrons use a less constrained set of 5' splice sites than standard introns as compared to the branchpoint and 3'ss sequences. This may reflect important interactions between the pre-mRNA cap binding complex and the U1 snRNP

248 during earliest steps of spliceosome assembly [55-58] and suggests these robust interactions allow
249 greater drift of the 5'ss than other splicing signals. This is also consistent with our observation that
250 26% of protointrons overlap 5' UTRs as compared with 5% for 3' UTRs and agrees with a
251 prediction of the intronization model developed for metazoans [8, 59]. We conclude that
252 protointrons use a wider variety of branchpoints and splice sites than do standard introns in *S.*
253 *cerevisiae* and hypothesize that protointrons may evolve toward standard intron status by acquiring
254 mutations that enhance the context and match to the consensus of the core splicing signals, in part to
255 increase their ability to compete with RPG pre-mRNAs [28].
256 With the exception of the protointrons found entirely within protein coding sequences,
257 typically at least one (and often all three) of the splicing signals for a given protointron in *S.*
258 *cerevisiae* is imbedded in sequence that is not conserved in closely related *Saccharomyces* species
259 (Fig 1B, E, Fig S1C, F). To analyze whether this is a distinguishing characteristic of protointrons,
260 we recorded the average phastCons score (range between 0, evolving as not conserved, and 1,
261 evolving as highly conserved, [60]) of the nucleotides within sequence windows containing the 5'ss,
262 the branchpoint, and the 3'ss of the standard introns and protointrons and plotted them (blue bars,
263 standard introns; orange bars, protointrons, Fig 2B). Many standard introns are embedded in
264 conserved protein coding sequences, and thus the splice sites and their immediate exon context are
265 also conserved, such that the average phastCons scores for both the 5' and 3'ss windows rise above
266 0.7 (Fig 2B). The branchpoints of standard introns are also conserved but have a broader and lower
267 score distribution, because constraining protein coding exon sequences are not usually found near
268 the branchpoints of standard introns. In contrast, the distributions of phastCons scores for each of
269 the protointron splicing signals is clearly bimodal, meaning that protointron splicing signals are
270 either highly conserved, falling within protein coding sequence, or are poorly conserved, falling in

271 UTRs or intergenic regions (Fig 2B). This distribution illuminates the sequence landscape within
272 which most protointrons arise. Since the strongly transcribed regions of the genome code mostly for
273 protein, and transcription is a prerequisite for splicing, protointrons tend to appear in or span less
274 well conserved noncoding RNA sequences such as UTRs and ncRNAs (Supplemental Figure S1B).
275 This distinguishes protointrons from standard introns and suggests that most of the protointrons we
276 detect have appeared only recently in the *S. cerevisiae* genome, when transcribed non-protein coding
277 regions acquire intron-like features by mutation.

278 Standard introns show a bimodal length distribution, with peaks at about 100 nt and 400 nt
279 ([61], Fig 2C). In contrast, the distribution of protointrons is on average shorter, with a single main
280 peak at around 100 nt in length, and few larger than 300 nt. These distributions are significantly
281 different (Kolmogorov-Smirnoff test, $p \leq 10^{-4}$), suggesting that if protointrons evolve into standard
282 introns, they may become longer by acquiring additional sequence features that enhance their
283 recognition by the spliceosome. Many of the larger standard introns are found in RPGs [61], where
284 secondary structures and other long distance RNA-RNA interactions promote efficient and accurate
285 splicing [62, 63]. The elaboration of such structures during evolution of increased splicing efficiency
286 may explain the increased intron length that characterizes the large intron class in yeast.

287 Protointrons are less efficiently spliced than standard introns (Fig 2D, Tables 1, S1 and S3).
288 The vast majority of standard introns are spliced at greater than 80% efficiency (median ~ 93%) by
289 comparison of splice junction reads to intron base coverage. Exceptions include meiotic introns
290 whose efficient splicing may require repression of RPGs or the expression of a meiosis-specific
291 splicing factor like Mer1 [27-29]. In contrast, most protointrons have splicing efficiencies below
292 20% at best (median ~ 1%). A few protointrons, such as the introns in the *S. cerevisiae MTR2*,
293 *USV1*, and *MCR1* genes or the *S. bayanus YTA12* gene, are uncharacteristically well spliced,

294 suggesting that they may be transitional intron forms or species-specific standard introns (see
295 below). Splicing improves for most protointrons and standard introns after rapamycin treatment,
296 however some standard introns appear to show reduced splicing, suggesting splicing repression in
297 response to rapamycin at those introns.
298
299 **Coding regions are depleted of sequences required for splicing**
300 Protointrons that emerge within coding regions (39%, Supplemental Figure S1B) might
301 disrupt gene expression by reducing mRNA levels or creating toxic proteins. Since protointrons
302 emerge readily from nonconserved sequence (Fig 2B), we wondered whether the appearance of
303 protointrons within ORFs most often reduces fitness, and thus whether the frequency of splice site
304 and branchpoint sequences might be lower than would be expected by chance in protein coding
305 regions. In rare cases such introns might allow advantageous mRNA regulation through NMD [5,
306 64] to emerge (as appears to have been the case with a recently evolved standard intron in *PRP5*,
307 [65]) or make mRNA for beneficial alternative proteins (as may be the case for *PTC7*, [30, 66, 67];
308 and *MRM2* [37], see below), which have in-frame conserved coding sequences through their introns.
309 Analysis of several diverged genomes by Farlow et al. revealed that the consensus 5' ss sequence is
310 significantly underrepresented in the coding strand of genes compared to the noncoding strand [68].
311 To test whether *S. cerevisiae* coding sequences might be depleted of splicing signals, we compared
312 their frequency in the ORF set of the extant *S. cerevisiae* genome with that in 10,000 synthetic ORF
313 sets derived by randomizing the order of codons for each ORF. This approach maintains ORF
314 length, integrity, GC content, and codon usage in the permuted ORF sets while generating partially
315 randomized nucleotide sequences that can be used as a background sequence set for comparison, and
316 has been used to evaluate co-evolution of RNA processing signals within coding sequence [69].

317 To assess the representation of 5' ss and branch point sequences, we chose two 6-mers as
318 proxies – one for the 5' ss (GTATGT), and one for the branch point (ACTAAC). We counted the
319 number of times each appeared in the extant S. cerevisiae ORF set, and in each of the 10,000
320 permuted ORF sets, and plotted them. For both 6-mers, their counts in the extant ORF set are less
321 than 3 standard deviations below the mean of their respective counts from the 10,000 permuted ORF
322 sets (vertical lines), indicating that these 6-mers are significantly underrepresented in the natural *S.*
323 *cerevisiae* coding sequences as compared to the randomized coding sequences (Fig 3A).
324 To determine whether these proxy 6-mers were unusually depleted as compared to other 6-
325 mers, we calculated a Z-score for each of the 4096 6-mer sequences in turn, comparing the counts of
326 each in the extant *S. cerevisiae* ORF set with its mean counts in the 10,000 permuted ORF sets, and
327 plotted the distribution (Fig 3B, grey bars). The intron branchpoint 6-mer "ACTAAC" is found
328 comparatively much less frequently in the extant genome than are other 6-mers (Fig 3B), and much
329 less frequently than the average stop codon-containing 6-mer (blue bars). The 5' ss 6-mer
330 "GTATGT" is also more depleted than the average 6-mer, especially when compared to the subset of
331 ATG containing 6-mers (maroon bars, Fig 3B). Because there is a large amount of information in
332 coding sequences, we cannot be certain the depletion of the splicing signal 6-mers is due to splicing.
333 Numerous other features are being randomized by the process of codon permutation, for example 6-
334 mer representation may be influenced by di-codon frequencies that affect translation [70]. Even so,
335 these observations are consistent with the idea that splicing signals within ORFs carry a risk of
336 reduced fitness. This suggests that a robust level of spliceosome activity may be sufficient to lead to
337 loss of correct mRNA should genetic drift create splice sites within ORFs, providing a rationale for
338 tight regulation of a splicing activity limited to pre-mRNAs that can compete [28].
339

Protointrons are idiosyncratic to closely related species

S. cerevisiae protointrons are not conserved in closely related yeasts, suggesting that they have appeared or disappeared in *S. cerevisiae* in the time since these lineages diverged. To explore the hypothesis that protointrons arise and disappear differently in the other *Saccharomyces* lineages, we treated cultures of *S. mikatae* and *S. bayanus* with rapamycin for 0 or 60 minutes, isolated RNA, depleted rRNA, and made cDNA libraries for sequencing. These strains are NMD competent (*UPF1*), so our ability to detect transcripts subject to NMD is limited. Regardless, nearly all annotated introns in *S. cerevisiae* are present in the *S. mikatae* and *S. bayanus* genomes, and *S. bayanus* has an additional standard intron in a *CHA4*-like gene that has no ortholog in *S. cerevisiae* (Tables S6 and S7). Some annotated *S. cerevisiae* introns are missing in these close relatives and based in part on their locations and splicing efficiencies, we propose reclassifying them as protointrons (see below). In contrast to the high conservation of standard intron locations, we detect distinct sets of protointrons in each species (Tables S6 and S7). We validated a subset of these (Fig 4) and find that most all of the *S. mikatae* protointrons are not present in either *S. cerevisiae* or *S. bayanus*, and that the *S. bayanus* protointrons are not found in *S. cerevisiae* or *S. mikatae* (Tables S3, S6, and S7). An exception to this is *YIL048W/NEO1*, in which the same protointron is observed in both *S. cerevisiae* (Table S3) and *S. mikatae* (Fig 4, Table S6). High sequence conservation in the coding region of *YIL048W/NEO1*, most likely due to functional constraints on the protein coding function of the sequence, has fortuitously preserved the splicing signals in all of the *Saccharomyces* yeasts. The intron is in frame with the coding sequence (Table S8), thus although the splicing of this protointron is not efficient, it remains possible this intron could generate a functional alternative protein. We conclude that protointrons are idiosyncratic in closely related yeast species. This is evidence for rapid evolutionary appearance and disappearance of sequences that can be functionally

363 recognized by the spliceosome. The dynamics of creation of protointrons thus appears consistent
364 with genetic drift, primarily in the rapidly evolving nonconserved sequences of recently diverged
365 genomes.
366
367 **Introns with features of both protointrons and standard introns may be intermediates in de**
368 **novo intron creation**
369 Based on the above analysis and those described elsewhere that note "novel" splicing [32-34,
370 37-39, 67], we propose defining standard introns as (1) conserved in related organisms or clades, (2)
371 efficiently spliced under appropriate physiological conditions, and (3) established in the pathway for
372 production or regulation of a functional gene product. Furthermore, we propose defining
373 protointrons as (1) not conserved in closely related species, (2) inefficiently spliced, and (3) not
374 clearly understood to contribute to correct expression or regulation of a gene. This simple definition
375 allows classification of most all of the observed splicing events in the yeast genome as either
376 protointron or standard intron, with only a few exceptions. The vast majority of protointrons arise
377 by neutral drift and likely provide no fitness advantage, and most probably disappear. A few introns
378 do not neatly fall into one or the other category and may be transitioning from protointron to
379 standard intron status, as predicted by the intronization model. Like protointrons these intermediate
380 class introns not conserved, but unlike typical protointrons they have increased splicing efficiency,
381 and may appear positioned to influence expression of the gene that carries them.
382 Examples of protointrons that may be on an evolutionary path toward standard intron status
383 include introns in the 5' UTRs of *S. cerevisiae MTR2, USV1, YEL023C*, and *MCR1*, and in the 5'
384 UTR of *S. bayanus YTA12* (Fig 5). Using the unrooted tree describing relationships between the
385 genomes of the sensu stricto yeasts [71], we map the appearance of these high efficiency

386 protointrons as predicted by their presence in extant genomes that have diverged over 10-20 million
387 years. The *MTR2* intron contains essential sequences [72] and can diversify the N-terminal sequence
388 of the mRNA export protein Mtr2 [73]. When sequences of related yeasts became available [31], it
389 became clear that the *MTR2* intron is unique to *S. cerevisiae* (Fig 5). High efficiency protointrons are
390 found in the 5'UTRs of *USV1* and *MCR1*. The *USV1* intron is efficiently spliced after rapamycin
391 treatment in *S. cerevisiae* and is also functional in *S. mikatae* (Fig 5, Table S6). However, *S.*
392 *kudiravzevii* and *S. bayanus* have different sets of nucleotide changes that eliminate splice sites and
393 branchpoints required for this intron. The *MCR1* intron is spliced at about 30%, and appears to be
394 shared by *S. paradoxus*, but is absent in *S. mikatae*, *S. bayanus*, and *S. kudriavzevii*. None of these
395 splicing events alter the N-terminus of Usv1 (a stress induced transcription factor) or Mcr1 (a
396 mitochondrial NADH-cytochrome b5 reductase), however both introns remove uORFs from the 5'
397 UTRs of these genes, suggesting that splicing could affect 5'UTR function in mRNA translation or
398 stability for both genes. Finally, a very efficiently spliced (>95%) intron is found in the 5'UTR of
399 the *S. bayanus YTA12* gene, as well as in *S. kudriavzevii* (Fig 5). Removal of this intron does not
400 alter the N-terminus of Yta12, a mitochondrial protein complex assembly factor [74], but does lead
401 to removal of a uORF. Interestingly the *S. cerevisiae YTA12* gene matches at 88 of 117 (75%)
402 positions in the *S. bayanus* intron and has neither an intron nor any uORF (see below).
403 Ten percent of the protointrons identified in *S. cerevisiae* are located exclusively in 5'UTRs
404 (Supplemental Figure S1B). The apparent relationship between introns and uORFs leads to the idea
405 that 5'UTR introns may be adaptive by protecting mRNAs with long 5'UTRs from the general
406 negative effect of uORFs [48, 75]. To test this idea, we asked whether uORFs are present more
407 frequently in 5'UTRs that contain standard introns, as compared to similarly sized 5'UTRs that do
408 not. There are 22 yeast genes (7%) with standard introns in their 5'UTRs, (this number does not

409 count the annotated introns in *MCR1*, *MTR2*, or *USV1*, which are not conserved across the *sensu*
410 *stricto* group). The size range of the (unspliced) 5'UTRs for these 22 is from ~240 to 950
411 nucleotides, and there are 91 intronless genes with 5'UTRs in this size range. We counted uORFs
412 longer than 4 codons (including the AUG, but not the stop codon) within 5'UTRs in this size range.
413 Among the 91 genes without 5' UTR introns, 53 lack any uORFs, whereas 38 have at least one
414 uORF. All 22 genes with 5'UTR introns have at least one uORF, and for 20 of these all the uORFs
415 in the 5' UTR are removed by splicing. This distribution of uORFs in 5'UTRs with introns is
416 unlikely to have been generated by chance (Fisher's exact test, $p < 10^{-5}$). One hypothesis to explain
417 this is that by removing much of the 5' UTR RNA, an intron may protect a gene that has a long
418 5'UTR from genetic drift that creates uORFs, or other translational inhibitory features like RNA
419 secondary structure [48]. Additional experiments will be needed to determine which if any of these
420 splicing events promotes gene expression and whether or not the effect contributes to fitness.
421 A second evolutionary scenario whereby protointrons may be adaptive concerns in frame
422 splicing, which would produce an alternative polypeptide. This appears to be the case for the
423 standard intron in *PTC7* [30, 66]. A similar intron is found in *MRM2*, where as many as three
424 different proteins may be produced (Tables S1 and S2, see also [37], NB: not annotated in SGD, but
425 this fits the standard intron definition). Despite forces that seem to deplete splicing signals within
426 ORFs (Fig 3), we find 20 (out of 63) 3n protointrons within ORFs that do not interrupt the reading
427 frame and thus could produce functional proteins, particularly under stress or other conditions where
428 RPG transcription is reduced (Table S8). We suggest that such protointrons provide evolutionary
429 opportunities to create new protein isoforms from existing genes.
430
431 **Telomeric Y' repeats**

Intron-like sequences have been noted in the telomeric Y' family of repeat sequences for more than 25 years and continue to be annotated in the Saccharomyces Genome Database (SGD). So far, molecular tests for splicing of these annotated introns have been negative [61, 76]. Intron predictions allow some Y' repeat element copies to encode a large (1838 amino acid) protein (e. g. YNL339C, Fig 6A), that carries an N-terminal Sir1 domain and a central DExD helicase domain. Other Y' elements differ in sequence and can only encode fragments of the open reading frame that may nonetheless produce smaller functional proteins, for example the helicase overexpressed in telomerase-deficient "escaper" colonies [76, 77]. The function(s) of any of the Y' element predicted proteins in normal cells are not known.

To determine if Y' element transcripts are spliced, we allowed RNAseq reads to map to the repetitive Y' elements (i. e. without masking). Although the mapped locations may not be the precise origin of the RNA that created the read, this allows us to identify spliced reads and assign them to possible members of the Y' repeat family. We find two introns within the Y' repeat family (Fig 6), one of which lies on the far left of the repeat and is required to create the open reading frame for the longest predicted protein (exemplified by YNL339C near TEL14L, Fig 6A). The other is in the center of the Y' repeat (exemplified by YLR464W near TEL12R, Fig 6B). Neither of these introns matches the annotations at SGD, and instead in both cases, downstream 3' ss are used (see also [37]). It is not uncommon for the yeast spliceosome to skip proximal 3' ss in favor of a distal 3' ss, in some cases due to secondary structure of the pre-mRNA [78]. The Y' elements in *S. cerevisiae* differ from each other; not all can express a protein as large as YNL399C after removal of intron 1 using the distal 3' ss. Intron 2 splicing does not greatly extend the open reading frame of YLR464W. To confirm that the reads arise from splicing rather than from a deleted copy of the Y' element precisely lacking the intron, we searched the genome using the "spliced" sequence produced for

455 intron 1 or intron 2 and found that there is no such contiguous genomic sequence. We conclude that
456 Y' element transcripts can carry at least two introns that are distinct from current annotations in SGD
457 (Fig 6).

458 To evaluate the sequence relationships of the Y' repeat element introns we aligned them with
459 each other, after merging identical copies into one. All the predicted intron 1 sequences have the
460 second most common 5' ss in the yeast genome (GUACGU, followed by the preferred A at position
461 7, [61]. The most distal 3' ss of several possible creates the large ORF, and is UAG for all except
462 YPR202W, which has a CAG. Several other potential 3' ss (including the one annotated in SGD)
463 are skipped or used alternatively. Interestingly only YPR202W, YRF1-3, YRF1-6, and YRF1-7 have
464 the canonical UACUAAC branch point sequence, whereas most of the others have UAUUAAC, a
465 variant found in some standard introns (Fig 6A). The remaining group (YEL075C, YRF1-2, and
466 YRF1-4) are deleted for the region containing the branch point, suggesting that they are unable to be
467 spliced. Intron 2 has the most common 5'ss GUAUGU, and the most common branch point
468 UACUAAC, and uses the first AAG (a less commonly used but standard 3' ss) downstream from the
469 branch site (Fig 6B). Most copies also contain an alternative 5' ss which is used less frequently. We
470 have not estimated the efficiency of splicing of these introns because we cannot reliably assign reads
471 to specific repeat elements with confidence. The current genome assemblies of *S. mikatae*, *S.*
472 *paradoxus*, and *S. kudriavzevii*, but not the *S. bayanus* assembly include at least one Y' element
473 related to the *S. cerevisiae* elements [71], but the precise numbers and arrangements of the Y'
474 elements in those genomes await refinement of the genome assemblies for those organisms.
475

476 **The *S. bayanus YTA12* protointron functions in *S. cerevisiae***

The finding of a highly efficient protointron in the *YTA12* 5' UTR of *S. bayanus* (and putatively in *S. kudriavzevii,* Fig 5) that is not observed in the alignable syntenic sequence of *S. cerevisiae* prompted us to test (1) whether this *S. bayanus*-specific intron can be spliced in *S. cerevisiae*, and (2) whether the intron might confer some advantage for growth on glycerol, given the function of Yta12 in assembly of mitochondrial protein complexes [74]. Fig 7A shows an alignment of the region including and upstream of the Yta12 start codon from *S. bayanus* (sacBay), *S. cerevisiae* (sacCer) and *S. cerevisiae* in which the 117 bp of the *S. cerevisiae* genome corresponding to the *S. bayanus* intron have been replaced in *S. cerevisiae* with the *S. bayanus* intron (Sc-SbI). This replacement was made using CRISPR/Cas9 guided cleavage of an *S. cerevisiae*-specific target sequence within the syntenic region and a repair fragment containing the *S. bayanus* intron (Fig 7B). As controls, we created *S. cerevisiae* strains precisely deleted for the syntenic region aligning with the *S. bayanus* intron, as well as versions of the *S. bayanus* intron with 5' ss mutations (Fig 7C). We isolated RNA and evaluated the expression of these modified *YTA12* genes by extension of a labeled primer complementary to *YTA12* mRNA with reverse transcriptase (Fig 7C). The major transcription start sites for *YTA12* in *S. cerevisiae* map about 300 nt from the 5' end of the primer (Fig 7A and C, lane 1). These start sites are unaffected by the 117 bp deletion (the same collection of cDNAs are shorter by 117 residues, lane 2). The migration of cDNAs from the deletion strain are useful to mark the expected position of spliced RNAs, and indeed replacement of the 117 bp with the *S. bayanus* intron sequence (lane 3) results in the appearance of the same collection of cDNAs with the disappearance of the signal from pre-mRNA, indicating efficient splicing (lane 3, compare with lane 1).

Mutation of the 5' ss from GUAUGU to GaAUGU or GaAcGU results in the reduction of the spliced mRNA cDNAs, and the appearance of cDNAs corresponding to pre-mRNA (lanes 4 and

5), indicating that splicing is inhibited by these mutations. Changing the 5' ss from GUAUGU to the less commonly used GUAcGU reduces the efficiency of splicing but does not block it, as judged by the slight accumulation of unspliced RNA (lane 6). Unexpectedly, the *S. bayanus* intron sequence activates a set of cryptic start sites in the *S. cerevisiae* sequences downstream of the major start site and the *S. bayanus* intron (Fig 7C, lanes 2-6). These start sites are inefficiently used in the wild type *S. cerevisiae YTA12* promoter (lane 1). One consequence is that new mRNAs are made that initiate downstream of the intron and thus do not require splicing for expression of Yta12. This interpretation is supported by the observation that all the strains grow on YP glycerol plates as well as wild type BY4741 (not shown). This result highlights the challenge of anticipating the effect of mutations in 5' UTRs where transcription, splicing, and translation operate together on the same sequence. This experiment measures changes in splicing due only to differences in the intron, and not due to any differences in exonic sequences or trans-acting factors between *S. bayanus* and *S. cerevisiae*. We conclude that the efficiently spliced protointron from *S. bayanus* is equally at home in *S. cerevisiae*. This intron appears to have formed in *S. bayanus* after *S. bayanus* and *S. cerevisiae* last shared a common ancestor, but before the divergence of *S. bayanus* from *S. kudriavzevii*.

Discussion

A second class of splicing events exposes roles of the spliceosome in evolution

Here we characterize a class of splicing events in yeast we call protointrons. Many previous studies have noted "novel" introns in yeast under a variety of experimental conditions and genetic backgrounds [32-39, 67]. Here we distinguish protointrons by several criteria, most importantly that they reside at locations not overlapping known standard introns. We first recognized protointrons while studying how the abrupt disappearance of RPG pre-mRNA during early nutrient deprivation

signaling frees the spliceosome to increase splicing of other pre-mRNAs [28, 29]. RNAseq analysis of NMD-deficient yeast cells treated with rapamycin revealed that protointrons are found throughout the transcriptome in both coding and non-coding regions of pre-mRNAs, ncRNAs, and antisense transcripts, such as CUTs, SUTs, and XUTs (Fig 1, Fig S1). Protointrons contain all of the splicing signals necessary for recognition by the spliceosome (5'SS, BP, and 3'SS), however the sequences of these signals are more variable than those of standard introns (Fig 2A and B). Whereas standard introns are conserved in related organisms, efficiently spliced, and established for production or regulation of a functional gene product, protointrons are present in one or a few closely related species, not efficiently spliced, and do not clearly contribute to correct expression or regulation of a gene. Given this redefinition, we propose a revised intron annotation, including the addition of a standard intron in *MRM2*, and molecular evidence for the correct location of expected but not demonstrated splicing of Y' repeat element transcripts. We provide this and related data on a publicly accessible genome browser with several *Saccharomyces* species genomes at http://intron.ucsc.edu/.

Splicing events that occur outside our expectation of what is needed to make a protein or a structural RNA have attracted labels like "splicing noise" or "splicing error" [79]. But viewing the spliceosome as an enzyme able to catalyze a complex series of pre-mRNA binding, refolding, and release operations, including two cleavage-ligation reactions, or even just the first one [35, 80], on a very diverse set of substrates (for review see [2]) suggests that such terms should be more carefully defined. The protointrons described here, as well as for example similar newly evolved splicing events observed in mammalian lncRNAs [81, 82] reveal the outer edges of the substrate repertoire of this enzyme in sequence space, and do not represent either splicing noise or splicing errors. We suggest the term "splicing noise" should refer to fluctuations due to stochastic events affecting

546 particular splicing events, just as the term "transcriptional noise" refers to the stochasticity of
547 transcription events (see [83] and references therein). We also suggest the term "splicing error"
548 should refer to events within the spliceosome that lead to spliceosome assembly or catalysis that is
549 incompatible with successful completion of the two splicing reactions, spliced product release, and
550 recycling. In order for splicing to contribute to rapid evolution of multicellular organisms it seems
551 likely that a variety of sequences besides highly evolved introns would need to be recognized and
552 spliced, including those that appear in genomes by genetic drift. The extent to which these
553 spliceosome-generated spliced RNA sequences contribute to fitness would eventually determine
554 their evolutionary fate. The protointron class of splicing substrates represents opportunity to create
555 new genes, create new proteins from existing genes, or impose new regulatory controls on existing
556 genes.
557
558 **Some protointrons show greater splicing efficiency and may be adaptive**
559 The forces and mechanisms that drive intron evolution in eukaryotic genomes are still largely
560 unknown. If protointrons represent raw material for intron creation by the process of intronization,
561 then perhaps the most efficiently spliced protointrons represent intermediates in standard intron
562 formation that are advancing by selection of improving mutations. Our data provide evidence for
563 rapid and complete intronization in the *YTA12* 5' UTR between now and the time *S. bayanus* and *S.*
564 *cerevisiae* last shared a common ancestor (~ 20 Mya, [71]). Over the 117 bp intron sequence, the *S.*
565 *cerevisiae* 5' UTR differs at 29 positions (Fig 7A). Replacement of this region with the *S. bayanus*
566 sequence produces an efficiently spliced intron in *S. cerevisiae* (Fig 7C). This intron transplantation
567 experiment shows that no species-specific barrier prevents this sequence from serving as an efficient
568 intron in *S. cerevisiae*. Although this intron appears fixed in the *S. bayanus* and *S. kudravzevii*

branch of the *Saccharomyces* tree, there is currently no evidence for fitness effects, and thus this intron could be a product of neutral evolution.

In some cases, a protointron might provide increased fitness that would explain its evolutionary persistence. We suggest three specific ways that protointrons may support improvements in gene function. Approximately 10% of protointrons reside entirely within 5'UTRs (Supplemental Figure S1B), including the four most efficiently spliced protointrons we observed (*S. cerevisiae MTR2*, *USV1*, and *MCR1*, *S. bayanus YTA12*). We realized that genes with long distances between their transcription start sites and their start codons (i. e. with large 5' UTRs) are at risk for mutations that create a uORF in the 5' UTR, which often negatively influences translation [48, 75]. Removal of a large region of the UTR by splicing would buffer this genetic risk. Secondary structures or other detrimental sequences that might arise in long 5'UTRs [84] might also be safely removed by splicing. To test the plausibility of this idea, we examined the frequency of uORFs in 5' UTRs of *S. cerevisiae* genes that have or do not have 5' UTR introns and found that uORFs are significantly more prevalent in 5' UTRs that have introns as compared to other 5' UTRs (see Results). This suggests that the presence of a 5' UTR intron may help buffer an mRNA against any detrimental effects of uORFs or RNA secondary structure, and provides evidence that intronization in particular in 5' UTRs may be adaptive in *Saccharomyces* species.

A second way that protointrons may become functional is by producing in frame splicing events within ORFs to create mRNAs encoding shorter protein isoforms with new functions. The frequency of splicing signals is lower than expected in *S. cerevisiae* ORFs (Fig 3), supporting the expectation that most introns that arise within ORFs would be detrimental to fitness. Despite this, we found 20 protointrons contained within ORFs that do not interrupt the reading frame, and that may lead to the translation of alternative protein products (Table S8). If such shorter proteins contribute

592 to fitness, mutations that increase the splicing of the protointron (without disrupting the function of
593 the full-length protein) may lead to the establishment and conservation of a standard intron that
594 allows production of both protein forms. This may be the mechanism by which the conserved in-
595 frame introns of *PTC7* [30, 66] and *MRM2* ([37], this work) have evolved. In these cases, both the
596 intron and the protein sequence encoded by the intron are conserved in *sensu stricto* yeasts,
597 suggesting both contribute to fitness across the genus *Saccharomyces*. Many protointrons span the
598 boundaries between conserved and nonconserved sequences (Fig 2B), increasing the chances that a
599 new splicing event will alter one or the other end of an existing protein. Studies of protein evolution
600 indicate that proteins evolve at their edges [85], suggesting that protointrons may contribute to this
601 as well. Although there is as yet no evidence for new function, the 5' UTR protointron in the *S.*
602 *cerevisiae MTR2* gene has arisen sufficiently close to the start codon that different alternative
603 splicing events add different peptides to the amino terminus of the annotated protein sequence [72,
604 73]. Thus, protointrons that appear in frame within existing genes, or that span the edges of existing
605 genes, create protein expression variation that may provide fitness advantages, in particular under
606 stress conditions that have yet to be explored.

607 A third way that protointrons may prove advantageous is through controlled downregulation
608 through splicing and NMD. We find that 16% of protointrons in *S. cerevisiae* span the 5' UTR and
609 coding region of twenty-seven genes and upon being spliced, remove the canonical AUG start codon
610 making these transcripts potential targets of NMD. In ten of these protointrons, the AUG start codon
611 is embedded within the GU**AUG** of the 5' ss (e. g. Ade2), suggesting sequences surrounding start
612 codons are particularly susceptible to drifting toward a 5' ss. A recently studied example of this is
613 the standard intron in the *PRP5* gene that is conserved in the *Saccharomyces* genus and destroys the
614 *PRP5* mRNA by removing the start codon and creating a transcript that is subject to NMD [65]. The

615 intron must have appeared since the divergence of the *Saccharomyces* species from their common
616 ancestor with *Lachancia kluveri*, since this more distant relative has a different intron in its *PRP5*
617 gene. This situation may evolve where overexpression of a particular protein may be detrimental.
618 *PRP5* encodes a splicing factor, and increase (or decrease) in Prp5 protein activity may increase
619 splicing and reduce (or decrease splicing and accumulate) *PRP5* mRNA levels by using this
620 conserved out of frame intron to create a homeostatic regulatory loop. A more difficult to recognize
621 but no less important mechanism is illustrated by the *BDF2* gene in which abortive splicing
622 downregulates expression through spliceosome-mediated decay [35]. It is unclear whether to
623 annotate this location and others like it [80] as an intron, since it does not appear that 3' splice site
624 selection is required or important for its activity. Thus, even protointrons that are out of frame within
625 coding regions, or pseudo-intron locations at which abortive splicing takes place may provide
626 opportunities for adaptive regulatory controls to evolve.
627
628 **Conclusions**
629 Protointrons are a rare class of splicing events that represent the action of the spliceosome on
630 RNA without a necessary connection to the expression of a mature gene. In mammalian cells the
631 spliceosome is no less constrained, and a very large number of alternative splicing events that appear
632 unrelated to "correct" gene expression support this [86]. In particular, newly evolved lncRNAs have
633 introns that are inefficiently spliced and have multiple alternative splice sites, unlike older, more
634 conserved lncRNA and mRNA encoding genes [81, 82]. These observations indicate that a general
635 feature of the evolution of introns is that any transcribed sequence has a chance of being spliced by
636 the spliceosome, should that sequence evolve recognizable splicing signals. Additionally, any
637 sequence that suddenly becomes transcribed can be expected to contain sequences by chance that are

638 immediately recognized as introns. Since the sequences required for splicing are ubiquitous and have
639 low information, many such newly appearing sequences will immediately produce diverse RNA
640 transcripts. If these confer some advantage, or if mutations that improve splicing become fixed by
641 neutral genetic drift, then a standard intron may evolve. This general pathway may be a source of
642 new introns whose splicing contributes to diversification of the transcriptome, and to the appearance
643 of new genes and new products from existing genes, as genomes evolve.
644

645 ## Materials and Methods

646 ### Strains and culture conditions

647 Two independent cultures of *S. cerevisiae* strain BY4741 *upf1Δ* (*MATa his3Δ1 leu2Δ0 met15Δ0*
648 *ura3Δ0 upf1Δ::KANMX*) were grown in YEPD medium at 30°C to an optical density at 600 nm
649 (OD_{600}) ≈ 0.5. The cultures were split and rapamycin was added to one half at a final concentration
650 of 200 ng/ml for 1 hour. *S. bayanus* strain JRY9195 (*MATa hoD::loxP his3 lys2 ura3*) and *S.*
651 *mikatae* strain JRY9184 (*MATa hoD::NatMX trp1D::HygMX ura3D::HygMX*) were grown in
652 YEPD medium at 26 °C, and were treated with rapamycin as for *S. cerevisiae* except at 26°C. These
653 strains were a kind gift of Chris Hettinger [71].
654

655 ### RNA isolation

656 RNA was extracted from yeast cells using Procedure 1 as described [87]. Prior to RNAseq library
657 construction (see below), RNA was DNased using Turbo DNase (Life Technologies) and RNA
658 quality was evaluated using the 2100 Bioanalyzer (Agilent).
659

660 ### RNAseq library preparation

5-10 ug of total *S. cerevisiae* RNA was depleted of ribosomal RNA using the RiboZero Gold rRNA Removal Kit (Illumina) according to the manufacturer's instructions. Strand-specific cDNA libraries were prepared using the Kapa Stranded RNA-Seq Library Preparation Kit for Illumina Platforms (Kapa Biosciences) following the manufacturer's instructions with the following modifications. Sequencing adapters and oligonucleotides used for PCR barcoding were from the NEBNext Multiplex Oligos for Illumina Kit (New England Biolabs, NEB). Prior to PCR amplification of the library, adapter-ligated cDNA was treated with USER enzyme (NEB). Adapter-ligated libraries were then PCR amplified for 10 cycles using NEB index primers compatible with Illumina sequencing. After amplification, size selection of the libraries was performed using an E-gel Safe Imager and 2% E-gel size select gels (Invitrogen). Indexed libraries were pooled and 100 bp paired-end sequenced on the same flow cell of an Illumina HiSeq4000 instrument at the Berkeley sequencing facility. RNA extracted from *S. bayanus and S. mikatae* was depleted of ribosomal RNA as described above. Strand-specific cDNA sequencing libraries were prepared as described [88] and 50 bp paired-end sequenced on the HiSeq2000 platform (Illumina).

Mapping and Analysis of RNAseq Data

RNAseq data is deposited in GEO under the accession number GSE102615. For *S. cerevisiae* libraries, all mappings were done using 100x100 bp reads to the SacCer3 Apr. 2011 genome assembly (Saccharomyces Genome Database, SGD, [89]). For *S. bayanus* and *S. mikatae* libraries, mappings were done using 51x51 bp reads to the SacBay2 and SacMik2 genome assemblies (Saccharomyces Sensu Stricto Database, [71]), respectively. Reads mapping by BowTie2 [90] to *S. cerevisiae* tRNA and rRNA defined by Ensemble or to Ty elements defined by SGD were discarded, however mappings to Y' elements were recovered. For each library, reads were remapped to their

684 respective genomes using STAR with two-pass mode [91]. PCR duplicate reads (reads with identical
685 positions at both ends) were discarded and reduced down to one read. Changes in gene expression
686 upon treatment of cells with rapamycin were determined using DESeq2 [92], comparing untreated
687 and treated cells. Splice junctions were identified by STAR mapping [91].

688 Splicing Indexes (ratios of splicing measurements) were calculated by comparing reads that
689 cross the intron, reads that cross the splice junction, and reads in exon 2 in different ways. Splice
690 junction coverage is taken as the number of reads that cross the splice junction. Intron coverage was
691 taken as the average per nucleotide coverage across the whole intron. When introns overlapped, a
692 minimal length intron was used such that start of the intron was the most downstream start of the
693 overlapping introns and the end was the most upstream start of the overlapping introns. Exon2
694 coverage was the average coverage for 100 bases of the following exon, using the most downstream
695 3' ss to define the exon. Log2-transformed ratios (Indexes) were calculated for the three
696 comparisons: intron/exon2, splice junction/exon2, splice junction/intron. Figure 1A shows how the
697 splice junction/intron index changes with rapamycin treatment by plotting the value of log2[splice
698 junction-60/intron-60] – log2[splice junction-0/intron-0] for each intron in each replicate. The
699 splicing events plotted here are for locations whose overall transcript level changes less than 2 fold,
700 and whose junctions are supported by at least 35 reads for standard introns or at least 50 reads for
701 protointrons. The general shift of the points to the upper right quadrant indicates increased splicing
702 efficiency (increased junction relative to intron reads) after rapamycin treatment.

703 Intron splice sites and candidate branch sits were extracted for analysis using the mapped
704 splice junctions and by choosing a best branch point using the following heuristics. The likely
705 branch points (underlined) were identified by searching introns for the following sequences in order
706 until a branchpoint was identified: 1. ACTA<u>A</u>, 2. RYTR<u>A</u>YR, 3. YTR<u>A</u>Y (where R = A or G, Y = C

or T) constrained to be 45 or more bases away from the 5' ss and no closer than 7 nucleotides upstream from the 3' ss. Candidate introns not matching YTRAY were considered to have no good match to a branchpoint consensus. If multiple equally good branchpoints are identified the one closer to the 3' ss was recorded. Details and scripts are at: <https://github.com/donoyoyo/intron_bp_generator>. To evaluate conservation, phastCons conservation scores were extracted from a window surrounding the splice site or branchpoint using data from the UCSC Human Genome Browser for *S. cerevisiae* at <http://genome.ucsc.edu>. Weblogos [93] were created using the site at https://weblogo.berkeley.edu.

Reverse Transcription and PCR

RNA was reverse transcribed using SuperScript III (Life Technologies) according to the manufacturer's instructions using a mixture of anchored oligo-dT (T24VN) and random hexamers as primer. Primers to validate and sequence products of splicing from protointrons by RT-PCR were designed using Primer3 [94]. PCR was performed using oligonucleotides listed in Table S5. PCR products were resolved by electrophoresis on agarose gels and visualized with ethidium bromide staining.

Cloning and Sanger sequencing of PCR products

PCR products generated by *T. aquaticus* DNA polymerase (Taq) were cut from low melting point agarose gels and purified using Machernary-Nagel gel extraction kits, then cloned using TOPO-cloning (Invitrogen). Inserts were sequenced by Sanger sequencing at the U. C. Berkeley sequencing center. Splice junctions were identified using BLAT [95] running behind a home copy of the UCSC Genome Browser [96] publicly available at http://intron.ucsc.edu/.

730

731 **Estimation of background frequency of splicing signals in codon-permuted yeast genes**

732 To test the hypothesis that "ACTAAC" (proxy for the branchpoint sequence), GTATGT
733 (proxy for the 5' ss), or any other 6-mer nucleotide sequence within extant yeast ORFs might be
734 enriched or depleted, we created 10,000 codon-permuted versions of the *S. cerevisiae* ORF set and
735 counted the number of each of the 4096 possible 6-mers in each, computing a Z-score for each that
736 compares representation of each in the extant ORF set to the mean representation of each in the
737 10,000 permuted ORF sets. To create permuted ORF sets in a way that preserves the GC content
738 and codon usage of the extant set, we permuted the codons within each ORF (except for the start and
739 stop codons) in the complete set of ORFs. Scripts for creating permuted ORF sets and analysis
740 related to this question can be found under this github link:
741 https://github.com/rshelans/genePermuter

742

743 **CRISPR/Cas9 mediated intron transplantation**

744 Yeast CRISPR editing was done essentially as described by DiCarlo et al [97], except that we
745 rearranged the elements from different plasmids into a simplified single plasmid system by Gibson
746 assembly. We obtained p426-crRNA-CAN1.Y and p414-TEF1p-Cas9-CYC1t [97] from Addgene.
747 To create a BaeI cleavable cassette for easy guide cloning, we annealed oligos newguide1 and
748 newguide2 together, and separately newguide3 and newguide4, and filled to make two fragments
749 which were mixed and then PCR amplified using newguide1 and newguide4 as primers (Table S5).
750 This duplex was purified and assembled using Gibson mix (NEB) with p426-crRNA-CAN1.Y that
751 had been cut with NheI and Acc65I to replace the CAN1.Y guide target region with a stuffer
752 fragment that could be released by BaeI (NEB) and allow any guide to be inserted easily (p426-

753 crRNA-BaeI). We then used p426-crRNA-BaeI as a template to amplify a fragment containing the
754 new cassette with the *SNR52* promoter and the *URA3* gene using oligos trp1-S-ura3 and Cyc-K-
755 SNR52 (Table S5). This fragment was combined with p414-TEF1p-Cas9-CYC1t that had been cut
756 with SnaBI and Acc65I and assembled using Gibson mix to create p416-TEF1p-Cas9-NLS-crRNA-
757 BaeI. The net effect of these manipulations is to (1) combine the guide RNA and Cas9 genes on a
758 single centromeric (low copy) plasmid, (2) create a flexible entry site for any guide sequence, and
759 (3) replace the *TRP1* marker with *URA3*. To target the *S. cerevisiae YTA12* 5'UTR, we cleaved
760 p416-TEF1p-Cas9-NLS-crRNA-BaeI with BaeI, annealed the YTA12_top YTA12_bot 25-mers
761 together (Table S5) and ligated them to the BaeI cleaved plasmid to produce p416-TEF1-Cas9-NLS-
762 CYC1t-crRNA-YTA12. The advantage of this single plasmid system is that guide sequences are
763 more easily inserted, only one plasmid is needed, and cells lacking the plasmid can be selected after
764 editing on 5-fluororotic acid (5-FOA) plates.

765 Rescue fragments were created by annealing combinations of synthetic oligonucleotides
766 (Table S5) and filling them in with DNA polymerase. These fragments contained the sequences
767 needed to edit the *S. cerevisiae YTA12* 5' UTR so that it contained the *S. bayanus* intron, or was
768 deleted of the intron-syntenic sequences, or contained different 5' ss mutations of the *S. bayanus*
769 intron. Candidate edited yeast clones were grown, and DNA was isolated and analyzed by PCR
770 using primers on either side of the edited site. PCR products were purified and sequenced at the U.
771 C. Berkeley sequencing center to confirm correct editing. Yeast strains determined to contain the
772 correct sequence were streaked on 5-FOA to select clones that have lost the p416-TEF1-Cas9-NLS-
773 CYC1t-crRNA-YTA12 plasmid.

774

775 **Acknowledgements**

Thanks very much to Joshua Arribere and Russ Corbett-Detig for insightful critical analysis of an earlier draft of this work. We appreciate Sam Fagg, Jen Quick-Cleveland, Stephanie Nystrom, and Santiago Sanchez for their constructive comments on this work. Thanks to Kevin Karplus for suggesting that codon-permutation could be used to create randomized ORF sets that preserve codon usage and GC content. We thank UCLA colleagues Tracy Johnson and Stephen Douglass for discussions and sharing results prior to publication. Thank you to Shana McDevitt and the Vincent J. Coates Genomics Sequencing Laboratory for advice on sequencing library preparation and for sequencing services.

References

1. Fica SM, Nagai K. Cryo-electron microscopy snapshots of the spliceosome: structural insights into a dynamic ribonucleoprotein machine. Nat Struct Mol Biol. 2017;24(10):791-9. Epub 2017/10/06. doi: 10.1038/nsmb.3463. PubMed PMID: 28981077.
2. Lee Y, Rio DC. Mechanisms and Regulation of Alternative Pre-mRNA Splicing. Annu Rev Biochem. 2015;84:291-323. Epub 2015/03/19. doi: 10.1146/annurev-biochem-060614-034316. PubMed PMID: 25784052; PubMed Central PMCID: PMCPMC4526142.
3. Scheres SH, Nagai K. CryoEM structures of spliceosomal complexes reveal the molecular mechanism of pre-mRNA splicing. Curr Opin Struct Biol. 2017;46:130-9. Epub 2017/09/10. doi: 10.1016/j.sbi.2017.08.001. PubMed PMID: 28888105.
4. Catania F, Lynch M. Where do introns come from? PLoS Biol. 2008;6(11):e283. Epub 2008/12/11. doi: 10.1371/journal.pbio.0060283. PubMed PMID: 19067485; PubMed Central PMCID: PMCPMC2586383.
5. Lynch M, Richardson AO. The evolution of spliceosomal introns. Curr Opin Genet Dev. 2002;12(6):701-10. PubMed PMID: 12433585.
6. Carmel L, Wolf YI, Rogozin IB, Koonin EV. Three distinct modes of intron dynamics in the evolution of eukaryotes. Genome Res. 2007;17(7):1034-44. Epub 2007/05/15. doi: 10.1101/gr.6438607. PubMed PMID: 17495008; PubMed Central PMCID: PMCPMC1899114.
7. Fink GR. Pseudogenes in yeast? Cell. 1987;49(1):5-6. Epub 1987/04/10. PubMed PMID: 3549000.
8. Catania F. From intronization to intron loss: How the interplay between mRNA-associated processes can shape the architecture and the expression of eukaryotic genes. Int J Biochem Cell Biol. 2017;91(Pt B):136-44. doi: 10.1016/j.biocel.2017.06.017. PubMed PMID: 28673893.
9. Yenerall P, Zhou L. Identifying the mechanisms of intron gain: progress and trends. Biol Direct. 2012;7:29. Epub 2012/09/12. doi: 10.1186/1745-6150-7-29. PubMed PMID: 22963364; PubMed Central PMCID: PMCPMC3443670.

10. Rogozin IB, Lyons-Weiler J, Koonin EV. Intron sliding in conserved gene families. Trends Genet. 2000;16(10):430-2. Epub 2000/10/26. PubMed PMID: 11050324.
11. Sorek R. The birth of new exons: mechanisms and evolutionary consequences. RNA. 2007;13(10):1603-8. Epub 2007/08/22. doi: 10.1261/rna.682507. PubMed PMID: 17709368; PubMed Central PMCID: PMCPMC1986822.
12. Worden AZ, Lee JH, Mock T, Rouze P, Simmons MP, Aerts AL, et al. Green evolution and dynamic adaptations revealed by genomes of the marine picoeukaryotes Micromonas. Science. 2009;324(5924):268-72. Epub 2009/04/11. doi: 10.1126/science.1167222. PubMed PMID: 19359590.
13. Collemare J, Beenen HG, Crous PW, de Wit PJ, van der Burgt A. Novel Introner-Like Elements in fungi Are Involved in Parallel Gains of Spliceosomal Introns. PLoS One. 2015;10(6):e0129302. Epub 2015/06/06. doi: 10.1371/journal.pone.0129302. PubMed PMID: 26046656; PubMed Central PMCID: PMCPMC4457414.
14. Collemare J, van der Burgt A, de Wit PJ. At the origin of spliceosomal introns: Is multiplication of introner-like elements the main mechanism of intron gain in fungi? Commun Integr Biol. 2013;6(2):e23147. Epub 2013/06/12. doi: 10.4161/cib.23147. PubMed PMID: 23750299; PubMed Central PMCID: PMCPMC3609843.
15. Simmons MP, Bachy C, Sudek S, van Baren MJ, Sudek L, Ares M, Jr., et al. Intron Invasions Trace Algal Speciation and Reveal Nearly Identical Arctic and Antarctic Micromonas Populations. Mol Biol Evol. 2015;32(9):2219-35. Epub 2015/05/23. doi: 10.1093/molbev/msv122. PubMed PMID: 25998521; PubMed Central PMCID: PMCPMC4540971.
16. Verhelst B, Van de Peer Y, Rouze P. The complex intron landscape and massive intron invasion in a picoeukaryote provides insights into intron evolution. Genome Biol Evol. 2013;5(12):2393-401. Epub 2013/11/26. doi: 10.1093/gbe/evt189. PubMed PMID: 24273312; PubMed Central PMCID: PMCPMC3879977.
17. van der Burgt A, Severing E, de Wit PJ, Collemare J. Birth of new spliceosomal introns in fungi by multiplication of introner-like elements. Curr Biol. 2012;22(13):1260-5. Epub 2012/06/05. doi: 10.1016/j.cub.2012.05.011. PubMed PMID: 22658596.
18. Lee S, Stevens SW. Spliceosomal intronogenesis. Proc Natl Acad Sci U S A. 2016;113(23):6514-9. doi: 10.1073/pnas.1605113113. PubMed PMID: 27217561; PubMed Central PMCID: PMCPMC4988565.
19. Li W, Tucker AE, Sung W, Thomas WK, Lynch M. Extensive, recent intron gains in Daphnia populations. Science. 2009;326(5957):1260-2. Epub 2009/12/08. doi: 10.1126/science.1179302. PubMed PMID: 19965475; PubMed Central PMCID: PMCPMC3878872.
20. Huff JT, Zilberman D, Roy SW. Mechanism for DNA transposons to generate introns on genomic scales. Nature. 2016. doi: 10.1038/nature20110. PubMed PMID: 27760113.
21. Irimia M, Rukov JL, Penny D, Vinther J, Garcia-Fernandez J, Roy SW. Origin of introns by 'intronization' of exonic sequences. Trends Genet. 2008;24(8):378-81. Epub 2008/07/04. doi: 10.1016/j.tig.2008.05.007. PubMed PMID: 18597887.
22. Sela N, Mersch B, Gal-Mark N, Lev-Maor G, Hotz-Wagenblatt A, Ast G. Comparative analysis of transposed element insertion within human and mouse genomes reveals Alu's unique role in shaping the human transcriptome. Genome Biol. 2007;8(6):R127. doi: 10.1186/gb-2007-8-6-r127. PubMed PMID: 17594509; PubMed Central PMCID: PMCPMC2394776.
23. Catania F, Schmitz J. On the path to genetic novelties: insights from programmed DNA elimination and RNA splicing. Wiley Interdiscip Rev RNA. 2015;6(5):547-61. doi: 10.1002/wrna.1293. PubMed PMID: 26140477.

857 24. Lopez PJ, Seraphin B. Genomic-scale quantitative analysis of yeast pre-mRNA splicing:
858 implications for splice-site recognition. RNA. 1999;5(9):1135-7. Epub 1999/09/25. PubMed PMID:
859 10496213; PubMed Central PMCID: PMCPMC1369835.
860 25. Ares M, Jr., Grate L, Pauling MH. A handful of intron-containing genes produces the lion's
861 share of yeast mRNA. RNA. 1999;5(9):1138-9. Epub 1999/09/25. PubMed PMID: 10496214;
862 PubMed Central PMCID: PMCPMC1369836.
863 26. Warner JR. The economics of ribosome biosynthesis in yeast. Trends Biochem Sci.
864 1999;24(11):437-40. Epub 1999/11/05. PubMed PMID: 10542411.
865 27. Munding EM, Igel AH, Shiue L, Dorighi KM, Trevino LR, Ares M, Jr. Integration of a
866 splicing regulatory network within the meiotic gene expression program of Saccharomyces
867 cerevisiae. Genes Dev. 2010;24(23):2693-704. Epub 2010/12/03. doi: 10.1101/gad.1977410.
868 PubMed PMID: 21123654; PubMed Central PMCID: PMCPMC2994042.
869 28. Munding EM, Shiue L, Katzman S, Donohue JP, Ares M, Jr. Competition between pre-
870 mRNAs for the splicing machinery drives global regulation of splicing. Mol Cell. 2013;51(3):338-
871 48. doi: 10.1016/j.molcel.2013.06.012. PubMed PMID: 23891561; PubMed Central PMCID:
872 PMCPMC3771316.
873 29. Venkataramanan S, Douglass S, Galivanche AR, Johnson TL. The chromatin remodeling
874 complex Swi/Snf regulates splicing of meiotic transcripts in Saccharomyces cerevisiae. Nucleic
875 Acids Res. 2017;45(13):7708-21. Epub 2017/06/24. doi: 10.1093/nar/gkx373. PubMed PMID:
876 28637241; PubMed Central PMCID: PMCPMC5570110.
877 30. Awad AM, Venkataramanan S, Nag A, Galivanche AR, Bradley MC, Neves LT, et al.
878 Chromatin-remodeling SWI/SNF complex regulates coenzyme Q6 synthesis and a metabolic shift to
879 respiration in yeast. J Biol Chem. 2017;292(36):14851-66. Epub 2017/07/26. doi:
880 10.1074/jbc.M117.798397. PubMed PMID: 28739803; PubMed Central PMCID:
881 PMCPMC5592666.
882 31. Kellis M, Patterson N, Endrizzi M, Birren B, Lander ES. Sequencing and comparison of
883 yeast species to identify genes and regulatory elements. Nature. 2003;423(6937):241-54. doi:
884 10.1038/nature01644. PubMed PMID: 12748633.
885 32. Gould GM, Paggi JM, Guo Y, Phizicky DV, Zinshteyn B, Wang ET, et al. Identification of
886 new branch points and unconventional introns in Saccharomyces cerevisiae. RNA.
887 2016;22(10):1522-34. Epub 2016/07/31. doi: 10.1261/rna.057216.116. PubMed PMID: 27473169;
888 PubMed Central PMCID: PMCPMC5029451.
889 33. Kawashima T, Douglass S, Gabunilas J, Pellegrini M, Chanfreau GF. Widespread use of
890 non-productive alternative splice sites in Saccharomyces cerevisiae. PLoS Genet.
891 2014;10(4):e1004249. doi: 10.1371/journal.pgen.1004249. PubMed PMID: 24722551; PubMed
892 Central PMCID: PMCPMC3983031.
893 34. Qin D, Huang L, Wlodaver A, Andrade J, Staley JP. Sequencing of lariat termini in S.
894 cerevisiae reveals 5' splice sites, branch points, and novel splicing events. RNA. 2016;22(2):237-53.
895 Epub 2015/12/10. doi: 10.1261/rna.052829.115. PubMed PMID: 26647463; PubMed Central
896 PMCID: PMCPMC4712674.
897 35. Volanakis A, Passoni M, Hector RD, Shah S, Kilchert C, Granneman S, et al. Spliceosome-
898 mediated decay (SMD) regulates expression of nonintronic genes in budding yeast. Genes Dev.
899 2013;27(18):2025-38. Epub 2013/09/26. doi: 10.1101/gad.221960.113. PubMed PMID: 24065768;
900 PubMed Central PMCID: PMCPMC3792478.
901 36. Aslanzadeh V, Huang Y, Sanguinetti G, Beggs JD. Transcription rate strongly affects
902 splicing fidelity and cotranscriptionality in budding yeast. Genome Res. 2018;28(2):203-13. Epub

903 2017/12/20. doi: 10.1101/gr.225615.117. PubMed PMID: 29254943; PubMed Central PMCID:
904 PMCPMC5793784.
905 37. Schreiber K, Csaba G, Haslbeck M, Zimmer R. Alternative Splicing in Next Generation
906 Sequencing Data of Saccharomyces cerevisiae. PLoS One. 2015;10(10):e0140487. Epub
907 2015/10/16. doi: 10.1371/journal.pone.0140487. PubMed PMID: 26469855; PubMed Central
908 PMCID: PMCPMC4607428.
909 38. Douglass S, Leung CS, Johnson TJ. Extensive Splicing across the Saccharomyces genome.
910 bioRxiv. 2019. doi: 10.1101/515163.
911 39. Miura F, Kawaguchi N, Sese J, Toyoda A, Hattori M, Morishita S, et al. A large-scale full-
912 length cDNA analysis to explore the budding yeast transcriptome. Proc Natl Acad Sci U S A.
913 2006;103(47):17846-51. Epub 2006/11/15. doi: 10.1073/pnas.0605645103. PubMed PMID:
914 17101987; PubMed Central PMCID: PMCPMC1693835.
915 40. Smith JE, Alvarez-Dominguez JR, Kline N, Huynh NJ, Geisler S, Hu W, et al. Translation of
916 small open reading frames within unannotated RNA transcripts in Saccharomyces cerevisiae. Cell
917 Rep. 2014;7(6):1858-66. doi: 10.1016/j.celrep.2014.05.023. PubMed PMID: 24931603; PubMed
918 Central PMCID: PMCPMC4105149.
919 41. Carvunis AR, Rolland T, Wapinski I, Calderwood MA, Yildirim MA, Simonis N, et al.
920 Proto-genes and de novo gene birth. Nature. 2012;487(7407):370-4. doi: 10.1038/nature11184.
921 PubMed PMID: 22722833; PubMed Central PMCID: PMCPMC3401362.
922 42. van Dijk EL, Chen CL, d'Aubenton-Carafa Y, Gourvennec S, Kwapisz M, Roche V, et al.
923 XUTs are a class of Xrn1-sensitive antisense regulatory non-coding RNA in yeast. Nature.
924 2011;475(7354):114-7. doi: 10.1038/nature10118. PubMed PMID: 21697827.
925 43. Xu Z, Wei W, Gagneur J, Perocchi F, Clauder-Munster S, Camblong J, et al. Bidirectional
926 promoters generate pervasive transcription in yeast. Nature. 2009;457(7232):1033-7. doi:
927 10.1038/nature07728. PubMed PMID: 19169243; PubMed Central PMCID: PMCPMC2766638.
928 44. Neil H, Malabat C, d'Aubenton-Carafa Y, Xu Z, Steinmetz LM, Jacquier A. Widespread
929 bidirectional promoters are the major source of cryptic transcripts in yeast. Nature.
930 2009;457(7232):1038-42. doi: 10.1038/nature07747. PubMed PMID: 19169244.
931 45. Ito T, Miura F, Onda M. Unexpected complexity of the budding yeast transcriptome. IUBMB
932 Life. 2008;60(12):775-81. doi: 10.1002/iub.121. PubMed PMID: 18649367.
933 46. Davis CA, Ares M, Jr. Accumulation of unstable promoter-associated transcripts upon loss of
934 the nuclear exosome subunit Rrp6p in Saccharomyces cerevisiae. Proc Natl Acad Sci U S A.
935 2006;103(9):3262-7. Epub 2006/02/18. doi: 10.1073/pnas.0507783103. PubMed PMID: 16484372;
936 PubMed Central PMCID: PMCPMC1413877.
937 47. Wyers F, Rougemaille M, Badis G, Rousselle JC, Dufour ME, Boulay J, et al. Cryptic pol II
938 transcripts are degraded by a nuclear quality control pathway involving a new poly(A) polymerase.
939 Cell. 2005;121(5):725-37. Epub 2005/06/07. doi: 10.1016/j.cell.2005.04.030. PubMed PMID:
940 15935759.
941 48. Arribere JA, Gilbert WV. Roles for transcript leaders in translation and mRNA decay
942 revealed by transcript leader sequencing. Genome Res. 2013;23(6):977-87. Epub 2013/04/13. doi:
943 10.1101/gr.150342.112. PubMed PMID: 23580730; PubMed Central PMCID: PMCPMC3668365.
944 49. He F, Jacobson A. Identification of a novel component of the nonsense-mediated mRNA
945 decay pathway by use of an interacting protein screen. Genes Dev. 1995;9(4):437-54. Epub
946 1995/02/15. PubMed PMID: 7883168.
947 50. Kandels-Lewis S, Seraphin B. Involvement of U6 snRNA in 5' splice site selection. Science.
948 1993;262(5142):2035-9. Epub 1993/12/24. PubMed PMID: 8266100.

51. Lesser CF, Guthrie C. Mutations in U6 snRNA that alter splice site specificity: implications for the active site. Science. 1993;262(5142):1982-8. Epub 1993/12/24. PubMed PMID: 8266093.
52. Roca X, Krainer AR. Recognition of atypical 5' splice sites by shifted base-pairing to U1 snRNA. Nat Struct Mol Biol. 2009;16(2):176-82. Epub 2009/01/27. doi: 10.1038/nsmb.1546. PubMed PMID: 19169258; PubMed Central PMCID: PMCPMC2719486.
53. Wu Q, Krainer AR. Splicing of a divergent subclass of AT-AC introns requires the major spliceosomal snRNAs. RNA. 1997;3(6):586-601. Epub 1997/06/01. PubMed PMID: 9174094; PubMed Central PMCID: PMCPMC1369508.
54. Parker R, Siliciano PG. Evidence for an essential non-Watson-Crick interaction between the first and last nucleotides of a nuclear pre-mRNA intron. Nature. 1993;361(6413):660-2. Epub 1993/02/18. doi: 10.1038/361660a0. PubMed PMID: 8437627.
55. Colot HV, Stutz F, Rosbash M. The yeast splicing factor Mud13p is a commitment complex component and corresponds to CBP20, the small subunit of the nuclear cap-binding complex. Genes Dev. 1996;10(13):1699-708. doi: 10.1101/gad.10.13.1699. PubMed PMID: 8682299.
56. Lewis JD, Izaurralde E, Jarmolowski A, McGuigan C, Mattaj IW. A nuclear cap-binding complex facilitates association of U1 snRNP with the cap-proximal 5' splice site. Genes Dev. 1996;10(13):1683-98. doi: 10.1101/gad.10.13.1683. PubMed PMID: 8682298.
57. Lewis JD, Gorlich D, Mattaj IW. A yeast cap binding protein complex (yCBC) acts at an early step in pre-mRNA splicing. Nucleic Acids Res. 1996;24(17):3332-6. doi: 10.1093/nar/24.17.3332. PubMed PMID: 8811086; PubMed Central PMCID: PMCPMC146107.
58. Schwer B, Shuman S. Conditional inactivation of mRNA capping enzyme affects yeast pre-mRNA splicing in vivo. RNA. 1996;2(6):574-83. PubMed PMID: 8718686; PubMed Central PMCID: PMCPMC1369396.
59. Lepennetier G, Catania F. mRNA-Associated Processes and Their Influence on Exon-Intron Structure in Drosophila melanogaster. G3 (Bethesda). 2016;6(6):1617-26. doi: 10.1534/g3.116.029231. PubMed PMID: 27172210; PubMed Central PMCID: PMCPMC4889658.
60. Siepel A, Bejerano G, Pedersen JS, Hinrichs AS, Hou M, Rosenbloom K, et al. Evolutionarily conserved elements in vertebrate, insect, worm, and yeast genomes. Genome Res. 2005;15(8):1034-50. Epub 2005/07/19. doi: 10.1101/gr.3715005. PubMed PMID: 16024819; PubMed Central PMCID: PMCPMC1182216.
61. Spingola M, Grate L, Haussler D, Ares M, Jr. Genome-wide bioinformatic and molecular analysis of introns in Saccharomyces cerevisiae. RNA. 1999;5(2):221-34. Epub 1999/02/19. PubMed PMID: 10024174; PubMed Central PMCID: PMCPMC1369754.
62. Howe KJ, Ares M, Jr. Intron self-complementarity enforces exon inclusion in a yeast pre-mRNA. Proc Natl Acad Sci U S A. 1997;94(23):12467-72. Epub 1997/11/14. PubMed PMID: 9356473; PubMed Central PMCID: PMCPMC25003.
63. Libri D, Stutz F, McCarthy T, Rosbash M. RNA structural patterns and splicing: molecular basis for an RNA-based enhancer. RNA. 1995;1(4):425-36. Epub 1995/06/01. PubMed PMID: 7493320; PubMed Central PMCID: PMCPMC1482409.
64. Farlow A, Meduri E, Dolezal M, Hua L, Schlotterer C. Nonsense-mediated decay enables intron gain in Drosophila. PLoS Genet. 2010;6(1):e1000819. doi: 10.1371/journal.pgen.1000819. PubMed PMID: 20107520; PubMed Central PMCID: PMCPMC2809761.
65. Karaduman R, Chanarat S, Pfander B, Jentsch S. Error-Prone Splicing Controlled by the Ubiquitin Relative Hub1. Mol Cell. 2017;67(3):423-32 e4. Epub 2017/07/18. doi: 10.1016/j.molcel.2017.06.021. PubMed PMID: 28712727.

66. Juneau K, Nislow C, Davis RW. Alternative splicing of PTC7 in Saccharomyces cerevisiae determines protein localization. Genetics. 2009;183(1):185-94. Epub 2009/07/01. doi: 10.1534/genetics.109.105155. PubMed PMID: 19564484; PubMed Central PMCID: PMCPMC2746143.

67. Zhang Z, Hesselberth JR, Fields S. Genome-wide identification of spliced introns using a tiling microarray. Genome Res. 2007;17(4):503-9. Epub 2007/03/14. doi: 10.1101/gr.6049107. PubMed PMID: 17351133; PubMed Central PMCID: PMCPMC1832097.

68. Farlow A, Dolezal M, Hua L, Schlotterer C. The genomic signature of splicing-coupled selection differs between long and short introns. Mol Biol Evol. 2012;29(1):21-4. doi: 10.1093/molbev/msr201. PubMed PMID: 21878685; PubMed Central PMCID: PMCPMC3245539.

69. Zhou Z, Dang Y, Zhou M, Yuan H, Liu Y. Codon usage biases co-evolve with transcription termination machinery to suppress premature cleavage and polyadenylation. Elife. 2018;7. Epub 2018/03/17. doi: 10.7554/eLife.33569. PubMed PMID: 29547124; PubMed Central PMCID: PMCPMC5869017.

70. Gamble CE, Brule CE, Dean KM, Fields S, Grayhack EJ. Adjacent Codons Act in Concert to Modulate Translation Efficiency in Yeast. Cell. 2016;166(3):679-90. Epub 2016/07/05. doi: 10.1016/j.cell.2016.05.070. PubMed PMID: 27374328; PubMed Central PMCID: PMCPMC4967012.

71. Scannell DR, Zill OA, Rokas A, Payen C, Dunham MJ, Eisen MB, et al. The Awesome Power of Yeast Evolutionary Genetics: New Genome Sequences and Strain Resources for the Saccharomyces sensu stricto Genus. G3 (Bethesda). 2011;1(1):11-25. Epub 2012/03/03. doi: 10.1534/g3.111.000273. PubMed PMID: 22384314; PubMed Central PMCID: PMCPMC3276118.

72. Parenteau J, Durand M, Veronneau S, Lacombe AA, Morin G, Guerin V, et al. Deletion of many yeast introns reveals a minority of genes that require splicing for function. Mol Biol Cell. 2008;19(5):1932-41. Epub 2008/02/22. doi: 10.1091/mbc.E07-12-1254. PubMed PMID: 18287520; PubMed Central PMCID: PMCPMC2366882.

73. Davis CA, Grate L, Spingola M, Ares M, Jr. Test of intron predictions reveals novel splice sites, alternatively spliced mRNAs and new introns in meiotically regulated genes of yeast. Nucleic Acids Res. 2000;28(8):1700-6. Epub 2000/03/29. PubMed PMID: 10734188; PubMed Central PMCID: PMCPMC102823.

74. Arlt H, Tauer R, Feldmann H, Neupert W, Langer T. The YTA10-12 complex, an AAA protease with chaperone-like activity in the inner membrane of mitochondria. Cell. 1996;85(6):875-85. Epub 1996/06/14. PubMed PMID: 8681382.

75. Brar GA, Yassour M, Friedman N, Regev A, Ingolia NT, Weissman JS. High-resolution view of the yeast meiotic program revealed by ribosome profiling. Science. 2012;335(6068):552-7. Epub 2011/12/24. doi: 10.1126/science.1215110. PubMed PMID: 22194413; PubMed Central PMCID: PMCPMC3414261.

76. Louis EJ, Haber JE. The structure and evolution of subtelomeric Y' repeats in Saccharomyces cerevisiae. Genetics. 1992;131(3):559-74. Epub 1992/07/01. PubMed PMID: 1628806; PubMed Central PMCID: PMCPMC1205030.

77. Yamada M, Hayatsu N, Matsuura A, Ishikawa F. Y'-Help1, a DNA helicase encoded by the yeast subtelomeric Y' element, is induced in survivors defective for telomerase. J Biol Chem. 1998;273(50):33360-6. Epub 1998/12/05. PubMed PMID: 9837911.

78. Meyer M, Plass M, Perez-Valle J, Eyras E, Vilardell J. Deciphering 3'ss selection in the yeast genome reveals an RNA thermosensor that mediates alternative splicing. Mol Cell.

2011;43(6):1033-9. Epub 2011/09/20. doi: 10.1016/j.molcel.2011.07.030. PubMed PMID: 21925391.

79. Pickrell JK, Pai AA, Gilad Y, Pritchard JK. Noisy splicing drives mRNA isoform diversity in human cells. PLoS Genet. 2010;6(12):e1001236. doi: 10.1371/journal.pgen.1001236. PubMed PMID: 21151575; PubMed Central PMCID: PMCPMC3000347.

80. Kannan R, Hartnett S, Voelker RB, Berglund JA, Staley JP, Baumann P. Intronic sequence elements impede exon ligation and trigger a discard pathway that yields functional telomerase RNA in fission yeast. Genes Dev. 2013;27(6):627-38. Epub 2013/03/08. doi: 10.1101/gad.212738.112. PubMed PMID: 23468430; PubMed Central PMCID: PMCPMC3613610.

81. Mele M, Mattioli K, Mallard W, Shechner DM, Gerhardinger C, Rinn JL. Chromatin environment, transcriptional regulation, and splicing distinguish lincRNAs and mRNAs. Genome Res. 2017;27(1):27-37. Epub 2016/12/09. doi: 10.1101/gr.214205.116. PubMed PMID: 27927715; PubMed Central PMCID: PMCPMC5204342.

82. Necsulea A, Soumillon M, Warnefors M, Liechti A, Daish T, Zeller U, et al. The evolution of lncRNA repertoires and expression patterns in tetrapods. Nature. 2014;505(7485):635-40. Epub 2014/01/28. doi: 10.1038/nature12943. PubMed PMID: 24463510.

83. Liu J, Martin-Yken H, Bigey F, Dequin S, Francois JM, Capp JP. Natural yeast promoter variants reveal epistasis in the generation of transcriptional-mediated noise and its potential benefit in stressful conditions. Genome Biol Evol. 2015;7(4):969-84. Epub 2015/03/13. doi: 10.1093/gbe/evv047. PubMed PMID: 25762217; PubMed Central PMCID: PMCPMC4419794.

84. Pickering BM, Willis AE. The implications of structured 5' untranslated regions on translation and disease. Semin Cell Dev Biol. 2005;16(1):39-47. Epub 2005/01/22. doi: 10.1016/j.semcdb.2004.11.006. PubMed PMID: 15659338.

85. Andreatta ME, Levine JA, Foy SG, Guzman LD, Kosinski LJ, Cordes MH, et al. The Recent De Novo Origin of Protein C-Termini. Genome Biol Evol. 2015;7(6):1686-701. doi: 10.1093/gbe/evv098. PubMed PMID: 26002864; PubMed Central PMCID: PMCPMC4494051.

86. Tress ML, Abascal F, Valencia A. Alternative Splicing May Not Be the Key to Proteome Complexity. Trends Biochem Sci. 2017;42(2):98-110. Epub 2016/10/08. doi: 10.1016/j.tibs.2016.08.008. PubMed PMID: 27712956.

87. Ares M. Isolation of total RNA from yeast cell cultures. Cold Spring Harb Protoc. 2012;2012(10):1082-6. Epub 2012/10/03. doi: 10.1101/pdb.prot071456. PubMed PMID: 23028070.

88. Yassour M, Pfiffner J, Levin JZ, Adiconis X, Gnirke A, Nusbaum C, et al. Strand-specific RNA sequencing reveals extensive regulated long antisense transcripts that are conserved across yeast species. Genome Biol. 2010;11(8):R87. Epub 2010/08/28. doi: 10.1186/gb-2010-11-8-r87. PubMed PMID: 20796282; PubMed Central PMCID: PMCPMC2945789.

89. Cherry JM, Hong EL, Amundsen C, Balakrishnan R, Binkley G, Chan ET, et al. Saccharomyces Genome Database: the genomics resource of budding yeast. Nucleic Acids Res. 2012;40(Database issue):D700-5. Epub 2011/11/24. doi: 10.1093/nar/gkr1029. PubMed PMID: 22110037; PubMed Central PMCID: PMCPMC3245034.

90. Langmead B, Salzberg SL. Fast gapped-read alignment with Bowtie 2. Nat Methods. 2012;9(4):357-9. Epub 2012/03/06. doi: 10.1038/nmeth.1923. PubMed PMID: 22388286; PubMed Central PMCID: PMCPMC3322381.

91. Dobin A, Davis CA, Schlesinger F, Drenkow J, Zaleski C, Jha S, et al. STAR: ultrafast universal RNA-seq aligner. Bioinformatics. 2013;29(1):15-21. Epub 2012/10/30. doi: 10.1093/bioinformatics/bts635. PubMed PMID: 23104886; PubMed Central PMCID: PMCPMC3530905.

92. Love MI, Huber W, Anders S. Moderated estimation of fold change and dispersion for RNA-seq data with DESeq2. Genome Biol. 2014;15(12):550. Epub 2014/12/18. doi: 10.1186/s13059-014-0550-8. PubMed PMID: 25516281; PubMed Central PMCID: PMCPMC4302049.
93. Crooks GE, Hon G, Chandonia JM, Brenner SE. WebLogo: a sequence logo generator. Genome Res. 2004;14(6):1188-90. Epub 2004/06/03. doi: 10.1101/gr.849004. PubMed PMID: 15173120; PubMed Central PMCID: PMCPMC419797.
94. Untergasser A, Cutcutache I, Koressaar T, Ye J, Faircloth BC, Remm M, et al. Primer3--new capabilities and interfaces. Nucleic Acids Res. 2012;40(15):e115. Epub 2012/06/26. doi: 10.1093/nar/gks596. PubMed PMID: 22730293; PubMed Central PMCID: PMCPMC3424584.
95. Kent WJ. BLAT--the BLAST-like alignment tool. Genome Res. 2002;12(4):656-64. Epub 2002/04/05. doi: 10.1101/gr.229202. PubMed PMID: 11932250; PubMed Central PMCID: PMCPMC187518.
96. Karolchik D, Barber GP, Casper J, Clawson H, Cline MS, Diekhans M, et al. The UCSC Genome Browser database: 2014 update. Nucleic Acids Res. 2014;42(Database issue):D764-70. Epub 2013/11/26. doi: 10.1093/nar/gkt1168. PubMed PMID: 24270787; PubMed Central PMCID: PMCPMC3964947.
97. DiCarlo JE, Norville JE, Mali P, Rios X, Aach J, Church GM. Genome engineering in Saccharomyces cerevisiae using CRISPR-Cas systems. Nucleic Acids Res. 2013;41(7):4336-43. Epub 2013/03/06. doi: 10.1093/nar/gkt135. PubMed PMID: 23460208; PubMed Central PMCID: PMCPMC3627607.

Figure Legends

Figure 1. Identification and Validation of Splicing at Unannotated Genomic Locations. RNA sequencing reads corresponding to spliced RNAs defined as described in the text were used to identify and measure splicing. Reads (~300M) were obtained from untreated cells and cells treated for 60 minutes with rapamycin from two biological replicate experiments. **(A)** Splicing efficiency of many introns improves after rapamycin treatment as judged by the log2 fold change in the ratio of splice junction reads to intron reads (splicing index; see Methods) for replicate experiments. Standard introns with ≥35 total junction reads are shown as blue dots. Unannotated and non-overlapping splicing events (protointrons) with ≥50 total junction reads are shown as orange dots. Data points in quadrant I indicate introns in which splicing improved after treatment with rapamycin in both replicate experiments. **(B)** Genomic alignment and lack of conservation for three example protointrons. Protointrons in a divergent upstream transcript *antiASH1*, a XUT *XUT12R-370*, and an

mRNA for *TAF13* are shown. The 5' ss is green, the branchpoint sequence is yellow, and the 3' ss is blue. The vertical bars indicate where additional intron sequences are not shown. **(C)** RT-PCR validation of protointron splicing and increased splicing after rapamycin is shown for the protointrons in (B), and for a non-coding vegetative cell transcript of a meiotic gene *ncSPO1*. PCR products corresponding in size to spliced (predicted based on RNAseq read structure) and unspliced RNAs are labeled. Splice junctions were confirmed by sequencing cloned PCR products. **(D)** Validation of protointron splicing through 5' ss not observed in standard introns. Junctions were validated by sequencing cloned PCR products. **(E)** A protointron in *SUT635* uses both GT-AG and AT-AC splice sites. The sequences of two cloned PCR products from *SUT635* are aligned to the genome (above) and the sequencing trace from the clone representing the use of AT-AC junctions is shown (below).

Figure 2. Differences between Standard Introns and Protointrons. (A) Splice site and branchpoint sequences of protointrons are less constrained in sequence than the standard introns. Weblogos representing position-specific weight matrices of the 5' ss, branch points, and 3' ss of the standard introns (top) and the protointrons (bottom) are shown. **(B)** The pattern of sequence conservation in the context of protointron splicing signals (orange bars in each panel) is bimodal as compared to the standard introns (blue bars in each panel). Histograms of the standard introns (blue bars) and the protointrons (orange bars) showing the distributions of PhastCons scores in windows containing the 5' ss, branchpoints, and 3' ss of the standard introns and protointrons. See text. **(C)** The size distribution of protointrons is distinct from that of the standard introns. Histograms show the distribution of intron sizes for the standard introns (blue bars) and the protointrons (orange bars). A Kolmogorov-Smirnoff test indicates the two distributions are different ($D = 0.22$, p value $\leq 10^{-4}$).

(D) Protointrons are much less efficiently spliced than standard introns. The scatter plot shows the relationship between splicing efficiency in untreated (time 0) cells and the change in splicing efficiency after one hour in rapamycin. Standard introns are shown in blue, protointrons in orange.

Figure 3. Hexamers representing splicing signals are depleted from annotated *S. cerevisiae* ORFs. **(A)** Histogram of counts of two hexamers (6-mers) serving as proxies for the branch point (ACTAAC, blue) and the 5' ss (GTATGT, yellow) in the extant ORF set of *S. cerevisiae* (vertical lines) as compared with the distribution of counts in each of 10,000 codon-permuted ORF sets. **(B)** Histogram of Z-scores computed for each of 4096 6-mers in the extant *S. cerevisiae* ORF set relative to their corresponding mean representation in 10,000 codon-permuted *S. cerevisiae* ORF sets. The number of 6-mers (y-axis) with the given Z-score (x-axis) is represented as a histogram in grey. Similar distributions are shown for two subclasses: those containing stop codons (blue histogram) and those containing start codons (maroon histogram). The Z-scores for the branchpoint proxy hexamer ACTAAC and the 5' splice proxy hexamer GTATGT are marked in the plot. The 6-mer "ACTAAC" had a Z-score of -12.25 and ranked 153rd lowest among all 4096 6-mers, and 91st lowest of 759 6-mers carrying stop codons. The 6-mer GTATGT had a Z-score of -6.98 and ranked 671st lowest among all 4096 6-mers, and 7th lowest of 255 6-mers carrying start codons.

Figure 4. Protointrons are found in other *Saccharomyces* species but are not conserved. RT-PCR products from RNA of *S. mikatae* (left) and *S. bayanus* (right) at different protointrons identified by RNAseq. Splice junctions were validated by cloning and sequencing the PCR products indicated by a white dot. Below the gel image are shown alignments of the RT-PCR product

1163 sequences from *S. mikatae antiYCR060W* and *S. bayanus YOL122C* to their corresponding genomes
1164 to show lack of conservation of splicing signals (boxed).
1165
1166 **Figure 5. Unusually efficient protointrons that may be evolving toward standard introns.**
1167 Positions of 5 efficiently spliced protointrons that share similarity with standard introns on the
1168 unrooted tree of sensu stricto *Saccharomyces* species are shown. Grey arrows indicate separation
1169 points that delineate boundaries between species having or lacking the indicated protointron
1170 sequence. Bars in the alignments indicate that sequences between these blocks are not shown. 5' ss
1171 are green, branchpoint sequences are yellow, and 3' ss are blue. Although these protointrons are
1172 restricted to one or two closely related species, their splicing efficiency approaches that of standard
1173 introns. Most protointrons are unique to a species and are very inefficiently spliced.
1174
1175 **Figure 6. Introns in the Y' element repeat family.** Two different introns are found in the
1176 transcribed Y' repeat elements. **(A)** Y' intron 1. Top: expanded view of the protein encoded by
1177 *YRF1-6* located in the Y' element at the left end of chromosome XIV with the Sir1 and DECD
1178 helicase homology regions indicated. An expanded segment from the upstream part of the gene
1179 shows the alignment of the detected intron relative to the annotated predicted intron at SGD. At the
1180 bottom is shown the alignment of the seven different versions of this intron from the seventeen Y'
1181 elements in the *S. cerevisiae* genome that possess it. Sequence names are based on standard and
1182 systematic annotations from the *Saccharomyces* Genome Database (SGD). 5' ss are green,
1183 branchpoint sequences are yellow, and 3' ss are blue. **(B)** Y' intron 2. Top: expanded view of the
1184 protein encoded by *YLR464W* located in the Y' element at the right end of chromosome XII. The
1185 alignment shows the detected intron relative to the annotated predicted intron at SGD. At the bottom

1186 is shown the alignment of the nine different versions of this intron from the nine Y' elements in the
1187 *S. cerevisiae* genome that possess it. Splicing signals are highlighted as in (A).
1188
1189 **Figure 7. The *S. bayanus* YTA12 5'UTR intron is efficiently spliced in *S. cerevisiae* (A)**
1190 Alignment of the *YTA12* promoter and 5'UTR from *S.cerevisiae* (sacCer, no intron), *S. bayanus*
1191 (sacBay, very efficient intron), and the *S. cerevisiae* strain carrying the *S. bayanus* intron (Sc-SbI),
1192 showing the major transcription start sites and the cryptic start sites (>), the splice sites (underlined),
1193 and the aligned base pairs (*). **(B)** Strategy for CRISPR/Cas9 editing-based transplantation of the *S.*
1194 *bayanus* intron into *S. cerevisiae*. A guide sequence was designed to recognize a sequence present in
1195 the *S. cerevisiae YTA12* 5'UTR but not present in the *S. bayanus* intron. A plasmid derived from
1196 those provided by DiCarlo et al. [97] expressing this guide along with Cas9 was co-transformed with
1197 a synthetic rescue fragment that contained the *S. bayanus* intron sequence between "exons" from *S.*
1198 *cerevisiae*. Repair of the double-stranded break using this rescue fragment results in transplantation
1199 of the *S. bayanus* intron into *S. cerevisiae*. **(C)** Reverse transcriptase primer extension analysis of
1200 RNA from the YTA12 locus of S. cerevisiae strains with the transplanted *S. bayanus* intron and
1201 mutant derivatives. The cDNAs representing unspliced (native) start sites, spliced (or deleted) RNAs
1202 initiating from the normal start site, and unspliced RNAs arising from cryptic start sites are indicated
1203 at left. Lane 1, wild type; lane 2, deletion of the region that aligns with the *S. bayanus* intron; lane 3,
1204 transplantation of the wild type S. bayanus intron; lane 4, GaAUGU mutation of the *S. bayanus*
1205 intron 5' ss; lane 5, GaAcGU mutant eliminating both the 5' ss and the start codon of a uORF; lane
1206 6, GUAcGU mutant that creates a common functional ss while removing the start codon of the
1207 uORF; lane m, 100 bp ladder markers.
1208

Supplemental Figure 1. (A) Coherence of gene expression changes after 60 minute rapamycin treatment between the two replicate experiments. Log2ratio of treatment to control read coverage over genes was plotted giving an R^2 value of ~0.99. Supplemental to Fig 1A. **(B)** Percentage of standard introns and protointrons that are located in non-coding, 5'UTR, 5'UTR^coding, coding, coding^3'UTR and 3'UTR regions. **(C)** Coverage tracks showing transcription through the genomic locus upstream of *ASH1* where the *antiASH1* protointron is located. Supplemental to Figs 1 B and C. **(D)** Coverage tracks showing transcription through the genomic locus upstream of *TUS1* where the *XUT12R-370* protointron is located. Supplemental to Figs 1 B and C. **(E)** Coverage tracks showing transcription through the genomic locus of *TAF13* where the *TAF13* protointron is located. Supplemental to Figs 1 B and C. **(F)** Coverage tracks showing transcription through the genomic locus of *SPO1* where the *ncSPO1* protointron is located. Supplemental to Figs 1 B and C. **(G)** Alignment of sequenced RT-PCR products showing the location of protointrons with unusual 5' ss. Supplemental to Fig 1D.

Table S1: *Saccharomyces cerevisiae* standard introns

Table S2: *Saccharomyces cerevisiae* overlapping standard introns

Table S3: *Saccharomyces cerevisiae* protointrons

Table S4: *Saccharomyces cerevisiae* filtered reads

Table S5: Oligonucleotides

Table S6: *Saccharomyces mikatae* introns

Table S7: *Saccharomyces bayanus* introns

Table S8: *Saccharomyces cerevisiae* in-frame protointrons

Talkish et al Fig 1

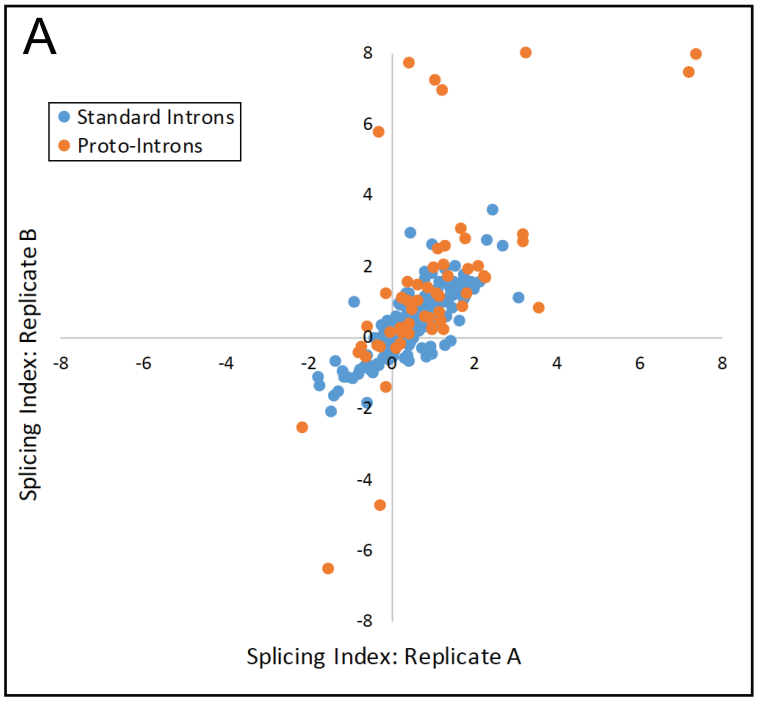

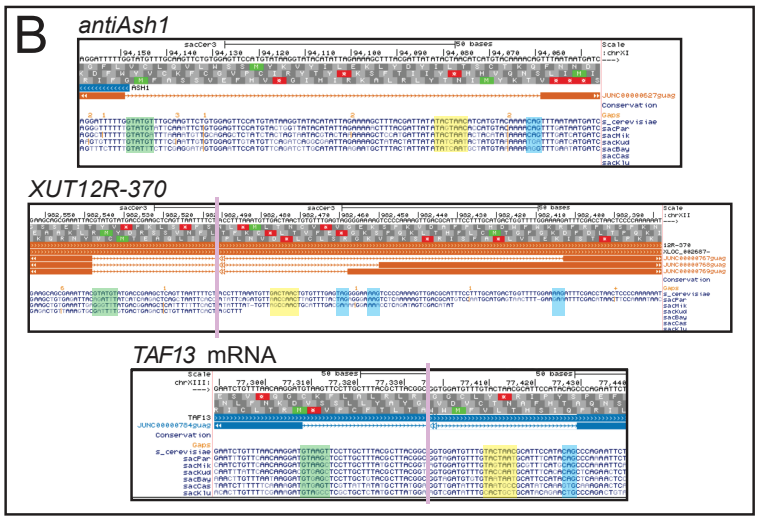

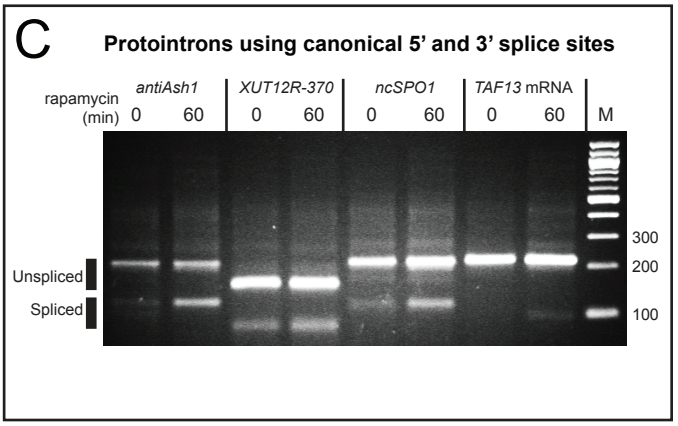

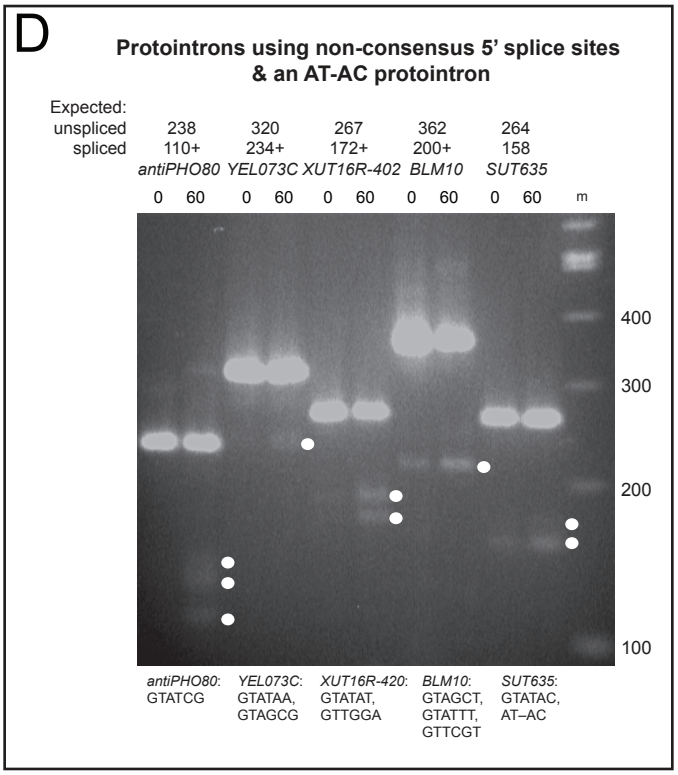

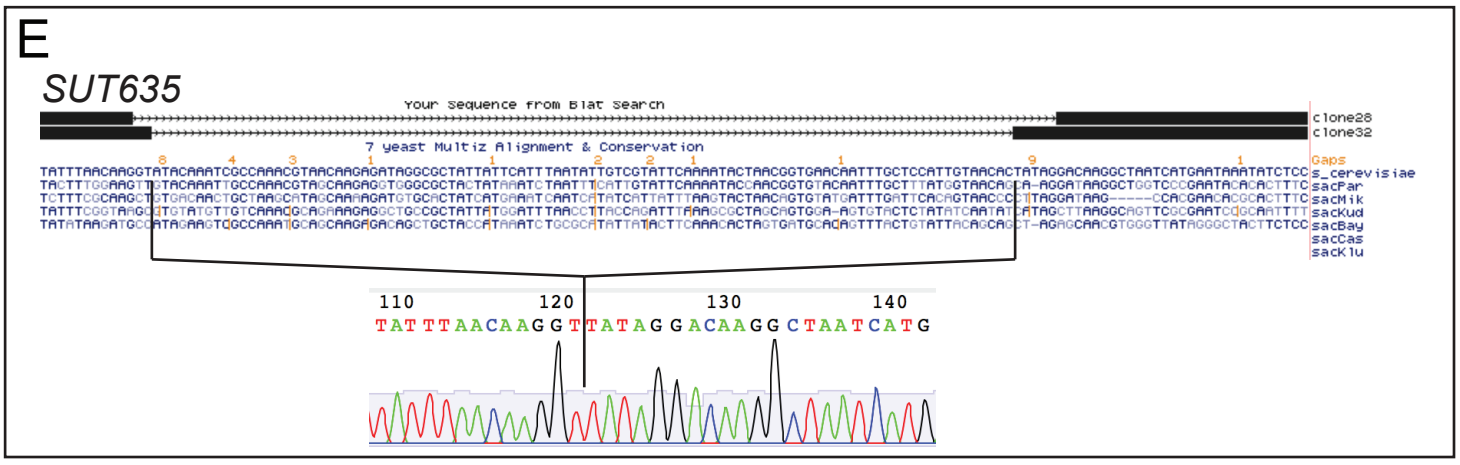

Talkish et al Fig 2

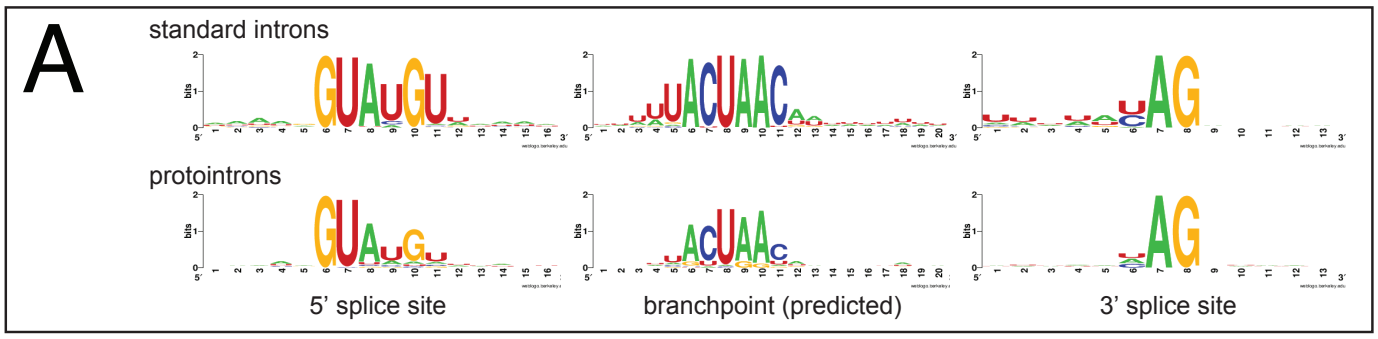

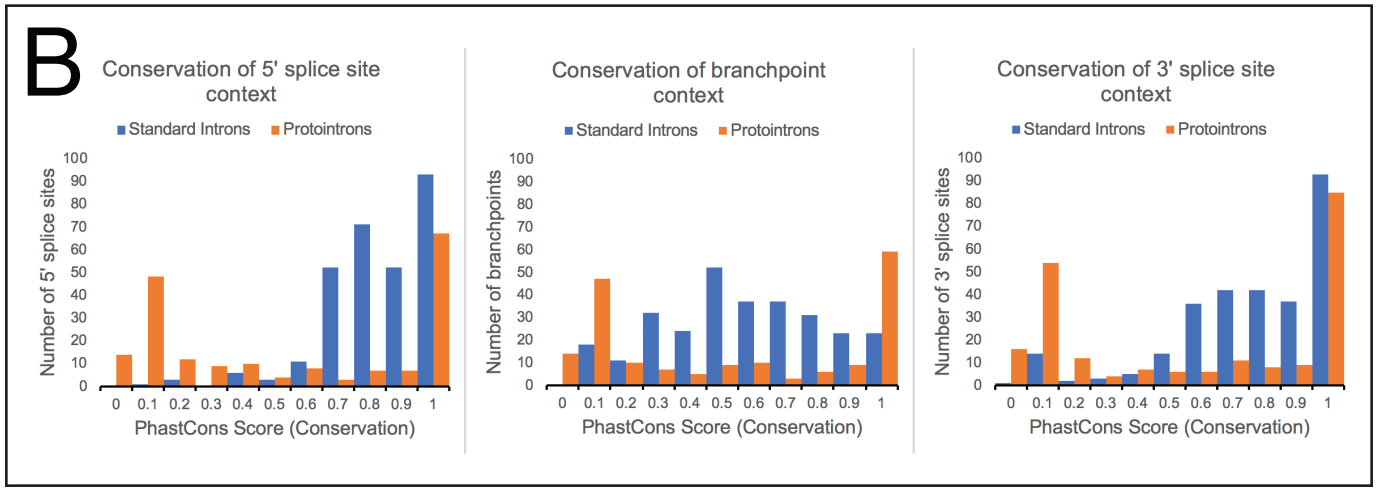

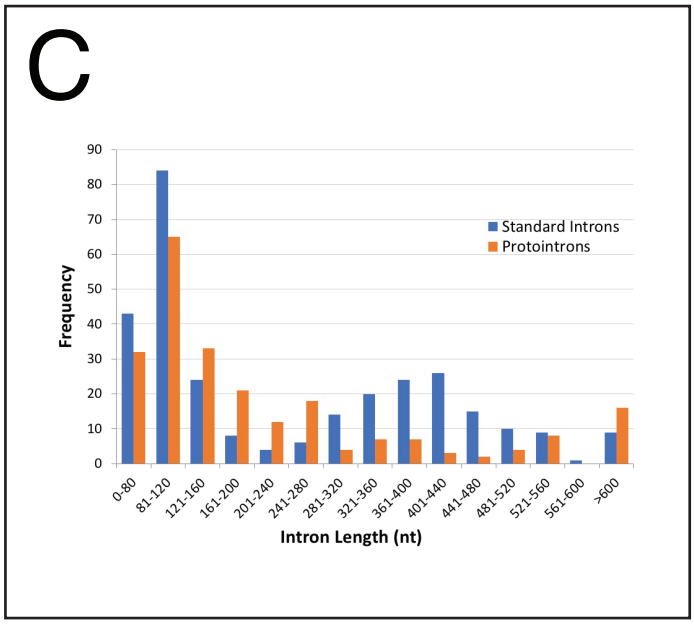

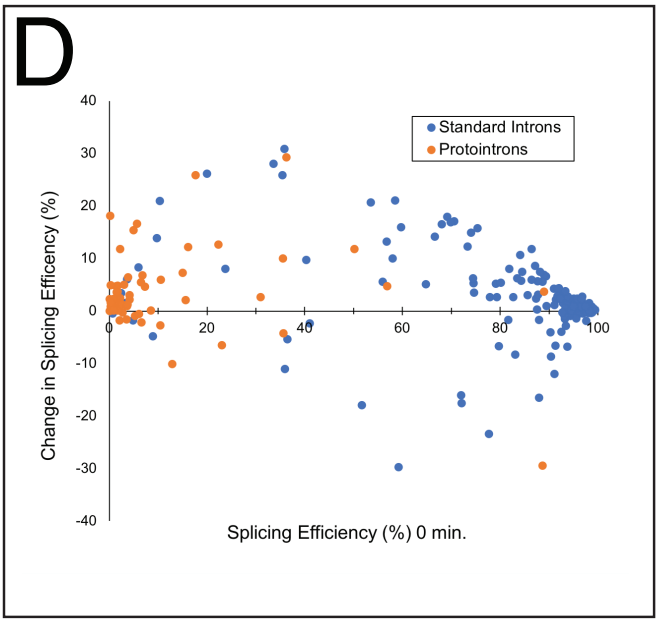

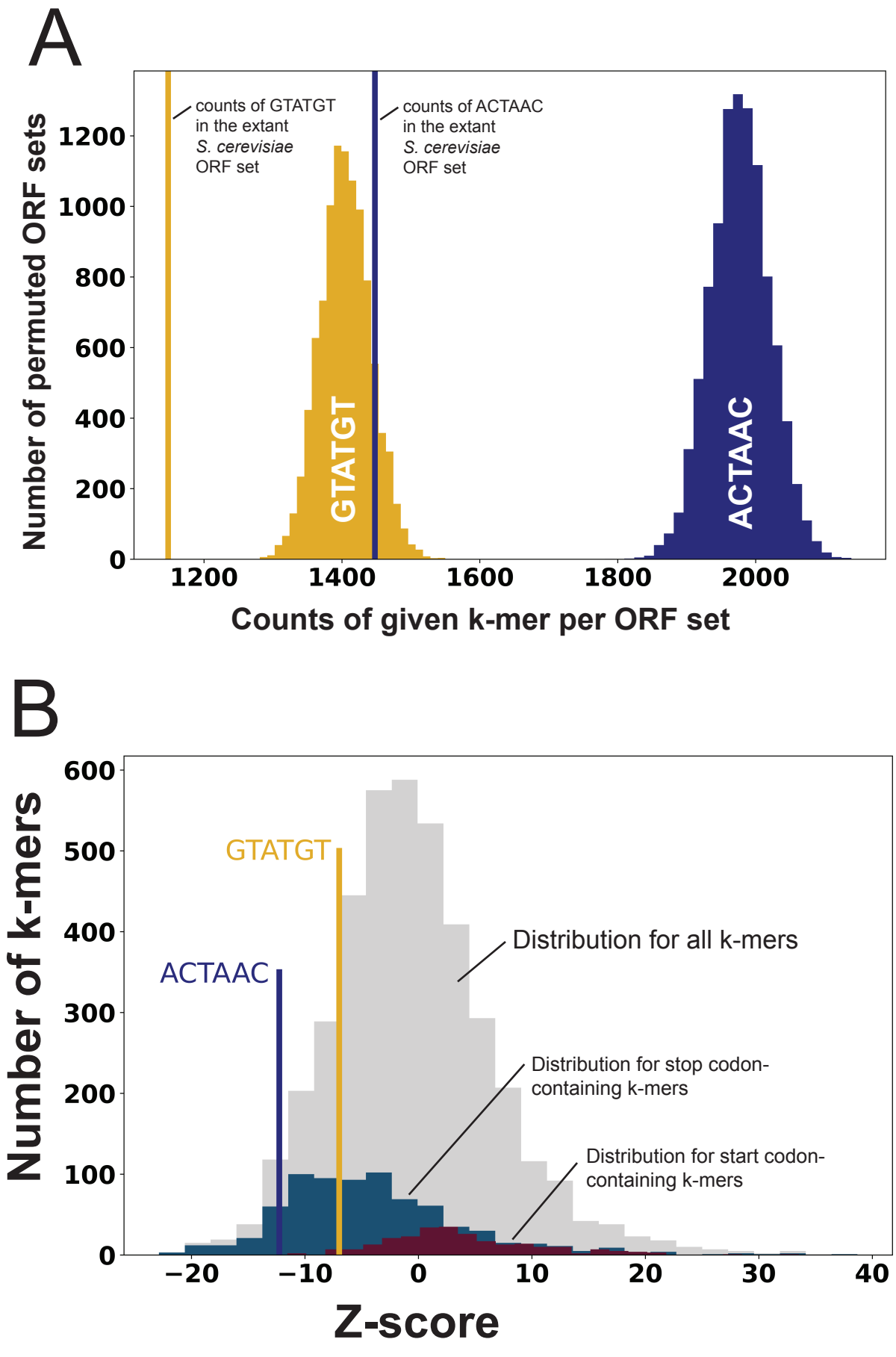

Talkish et al Fig 4

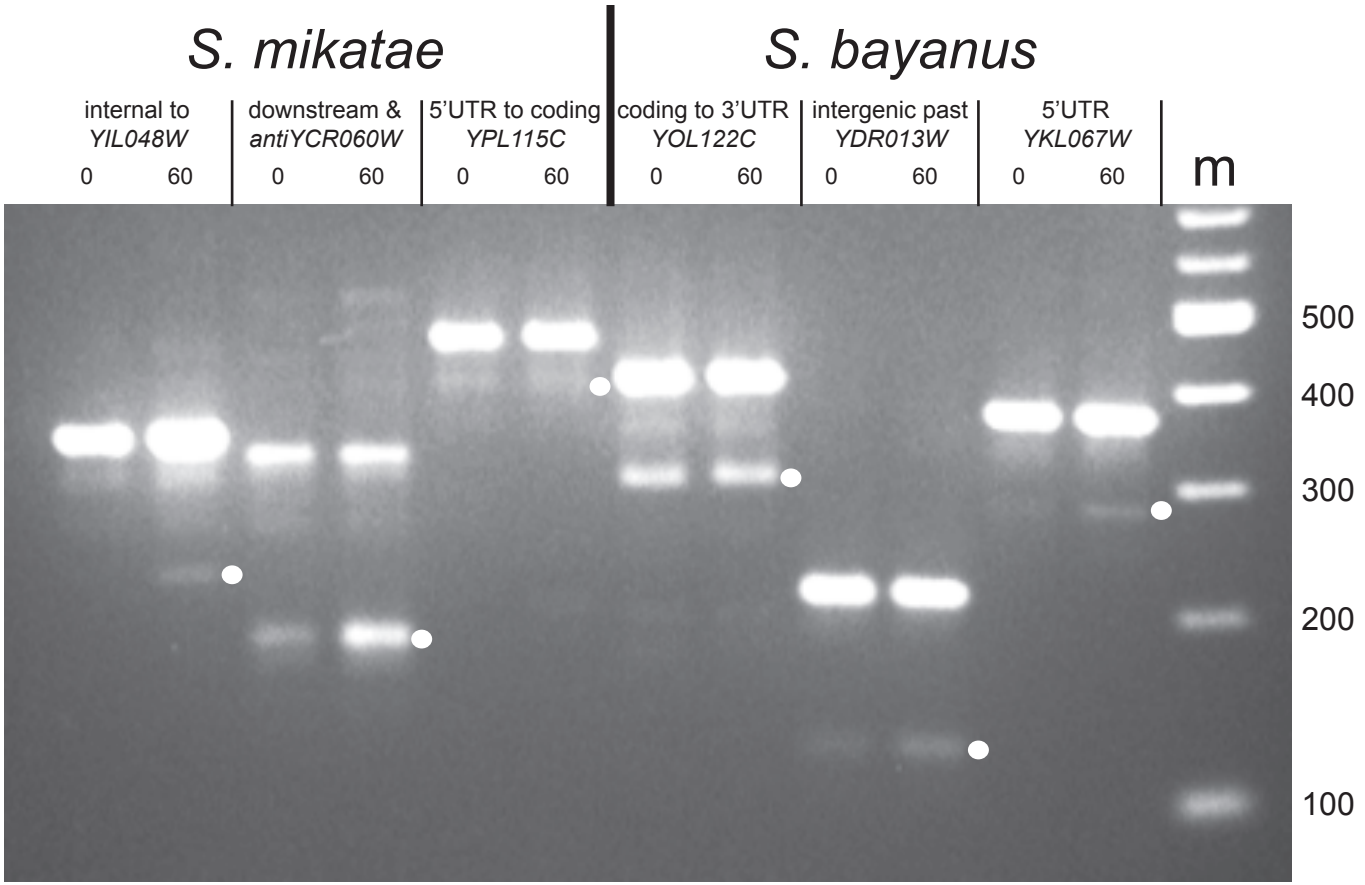

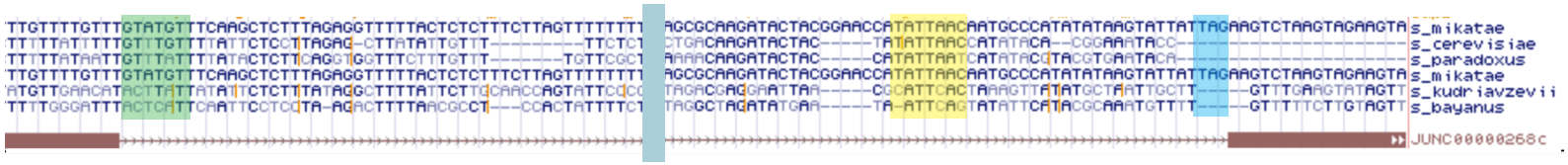

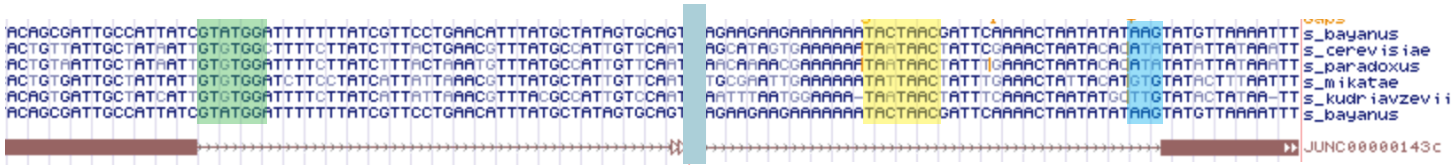

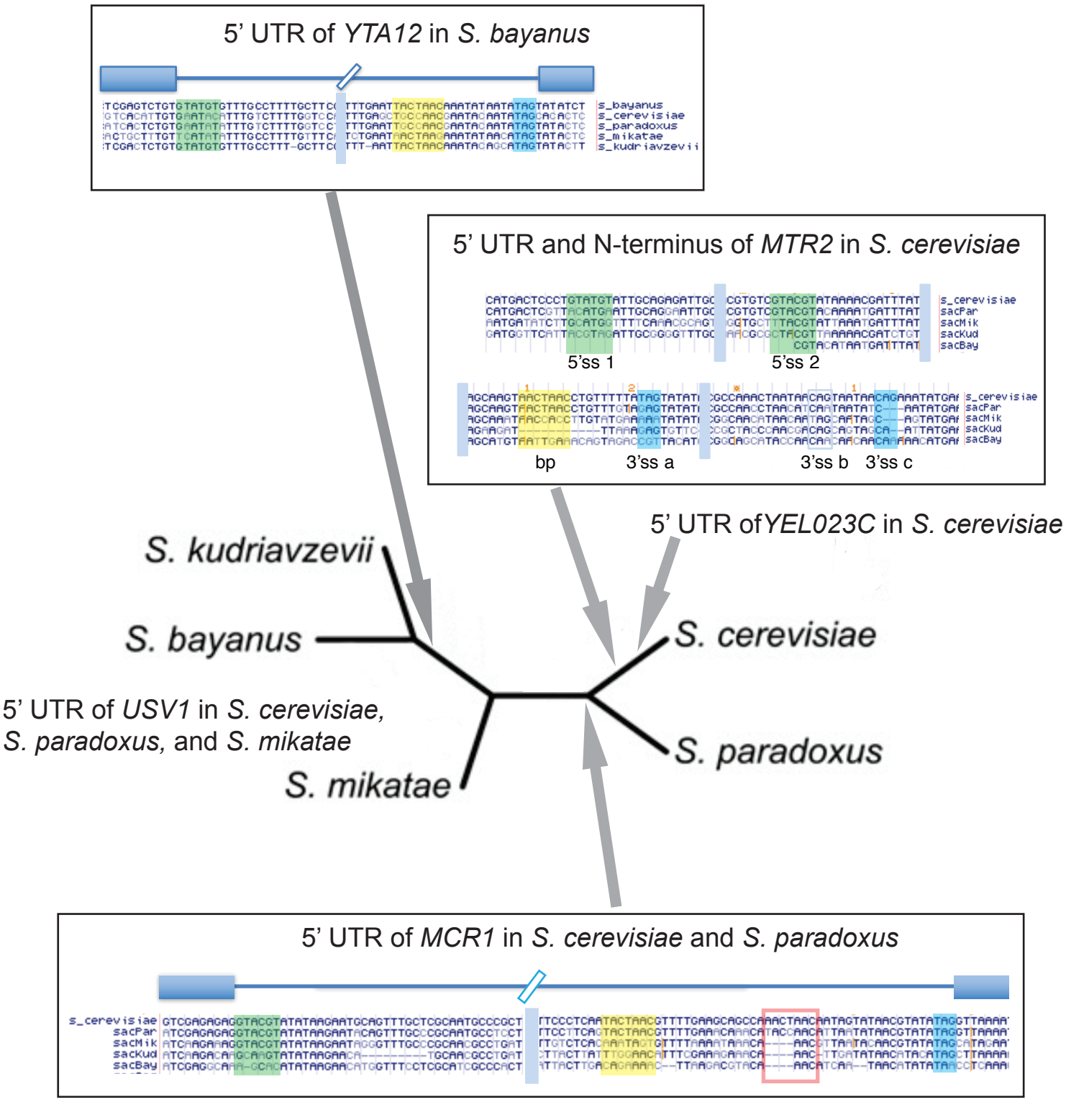

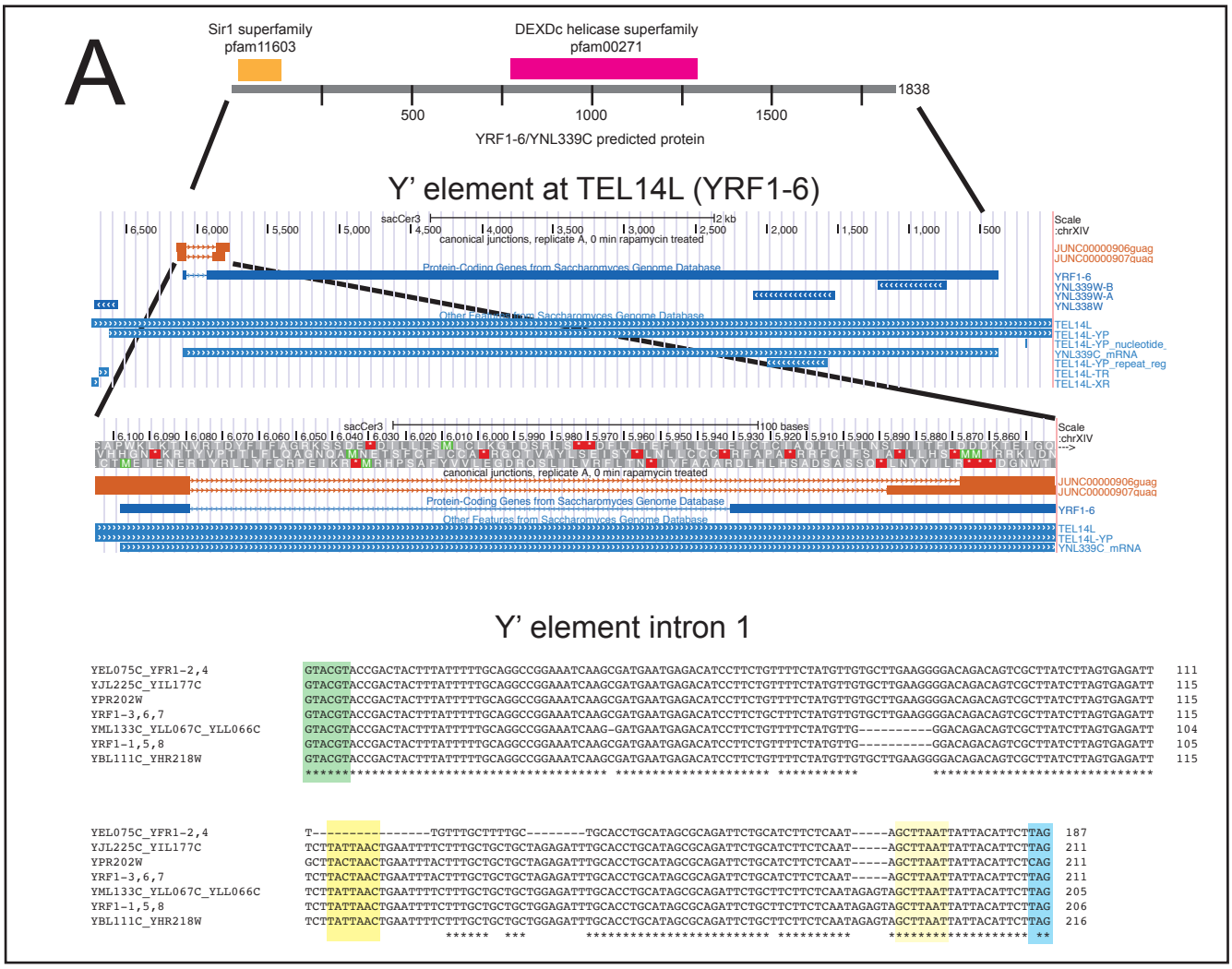

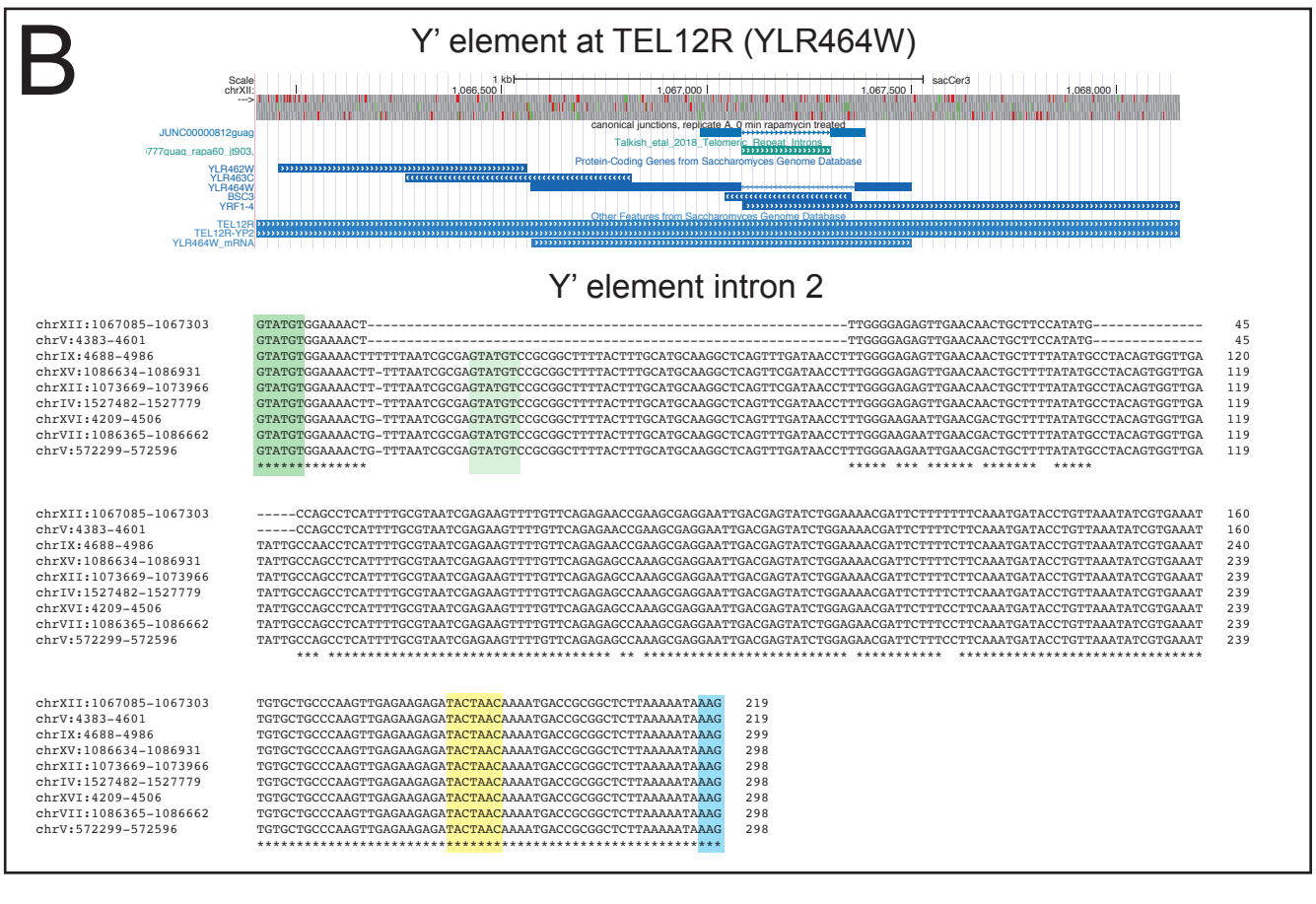

Talkish et al Fig 7